Available online at www.sciencedirect.com
ScienceDirect
Lithos 91 (2006) 229–249
LITHOS
www.elsevier.com/locate/lithos

The mineral isotope composition of two Precambrian carbonatite complexes from the Kola Alkaline Province – Alteration versus primary magmatic signatures

M. Tichomirowa [a,*], G. Grosche [a], J. Götze [a], B.V. Belyatsky [b], E.V. Savva [b], J. Keller [c], W. Todt [d]

[a] *Institute of Mineralogy, Technische Universität Bergakademie Freiberg, Brennhausgasse 14, D-09599 Freiberg, Germany*
[b] *Institute of Precambrian Geology and Geochronology, Russian Academy of Sciences, nab Makarova 2, 199034 St. Petersburg, Russia*
[c] *Institute of Mineralogy, Petrology and Geochemistry, University Freiburg, Albertstr. 23b D-79104 Freiburg, Germany*
[d] *Max-Planck-Institute of Chemistry, Department Geochemistry, P.O. Box 3060, D-55020 Mainz, Germany*

Received 4 July 2005; accepted 13 March 2006
Available online 23 June 2006

Abstract

We investigated the isotope composition (O, C, Sr, Nd, Pb) in mineral separates of the two Precambrian carbonatite complexes Tiksheozero (1.98 Ga) and Siilinjärvi (2.61 Ga) from the Karelian–Kola region in order to obtain information on Precambrian mantle heterogeneity. All isotope systems yield a large range of variations. The combination of cathodoluminescence imaging with stable and radiogenic isotopes on the same samples and mineral separates indicates various processes that caused shifts in isotope systems. Primary isotope signatures are preserved in most calcites (O, C, Sr, Pb), apatites (O, Sr, Nd), amphiboles (O), magnetites (O), and whole rocks (Sr, Nd).

The primary igneous C and O isotope composition is different for both complexes (Tiksheozero: $\delta^{13}C=-5.0‰$, $\delta^{18}O=6.9‰$; Siilinjärvi: $\delta^{13}C=-3.7‰$, $\delta^{18}O=7.4‰$) but very uniform and requires homogenization of both carbon and oxygen in the carbonatite melt. The lowest Sr isotope ratios of our carbonates and apatites from the Archaean Siilinjärvi (0.70137) and the Palaeoproterozoic Tiksheozero (0.70228) complexes are in the range of bulk silicate earth (BSE). Positive ε_{Nd} values of the two carbonatites point to very early Archaean enrichment of Sm/Nd in the Fennoscandian mantle. No HIMU components could be detected in the two complexes, whereas Tiksheozero carbonatites give the first indication of Palaeoproterozoic U depletion for Fennoscandia.

Sub-solidus exchange processes with water during emplacement and cooling of carbonatites caused an increase in the oxygen isotope composition of some carbonates and probably also an increase of their $^{87}Sr/^{86}Sr$ ratio. A larger increase of initial Sr isotope ratios was found in carbonatized silicic rocks compared to carbonatite bodies. The Svecofennian metamorphic overprint (1.9–1.7 Ga) caused reset of Rb/Sr (mainly mica) and Pb/Pb (mainly apatite) isochron systems.

Keywords: Carbonatite; C–O–Sr–Nd–Pb isotopes; Mantle source; Kola Alkaline Province; Mantle heterogeneity

* Corresponding author. Tel.: +49 3731 393528; fax: +49 3731 393129.
E-mail address: tichomir@mineral.tu-freiberg.de (M. Tichomirowa).

0024-4937/$ - see front matter © 2006 Elsevier B.V. All rights reserved.
doi:10.1016/j.lithos.2006.03.019

1. Introduction

Isotope studies (O, C, Sr, Nd, Pb) of carbonatites characterize their mantle source. Young carbonatites (<400 Ma) have similar radiogenic isotope compositions to ocean island basalts (OIB) and are often thought to be induced by deep mantle plumes (e.g., Nelson et al., 1988; Bell, 1998; Bell and Tilton, 2001; Bell and Rukhlov, 2004). These carbonatites form mixing lines in Sr–Nd–Pb isotope diagrams (e.g., Bell and Blenkinsop, 1989) generally lying between the EM I (enriched mantle 1) and HIMU (high μ; $\mu = {}^{238}U/{}^{204}Pb$) mantle isotope endmembers. Kramm (1993) first defined a linear array in Nd–Sr isotope space for carbonatites from the Kola Alkaline Province (KAP) known as the Kola Carbonatite Line.

Old carbonatites are especially interesting for understanding the isotope evolution of the mantle from Precambrian time to present. Investigations of Canadian and African alkaline complexes have shown systematic changes in their isotope composition with their emplacement time while Archaean carbonatites cluster around the estimated ratios for bulk silicate Earth (e.g., Tilton and Bell, 1994). However, Rukhlov et al. (2001) and Bell and Rukhlov (2004) concluded that mantle heterogeneity was already present in Archaean time based on Sr–Nd isotope data of carbonatites from Canada, Fennoscandia and Greenland.

Therefore, precise isotope data of Precambrian carbonatites are important for the discussion of the presence and evolution of mantle heterogeneities. Effects of sub-solidus exchange and post-magmatic processes which can lead to significant shifts in isotope signatures of carbonatites and alkaline rocks should be considered for this discussion (e.g., Sindern and Kramm, 2000; Bühn et al., 2003; Marks et al., 2003; Halama et al., 2005).

In the present study we carried out a combined and detailed investigation on two Precambrian carbonatite complexes (Siilinjärvi, Tiksheozero) including optical and cathodoluminescence microscopy, stable (O, C) and radiogenic (Sr, Nd, Pb) isotope composition of mineral phases and whole rock samples. The primary magmatic isotope composition is used for the discussion of mantle source and mantle heterogeneities. Special emphasis is given to the discussion of the influence of sub-solidus exchange processes with water as well as metamorphic processes on shifts in the isotope composition.

2. Geology and samples

2.1. Tiksheozero carbonatite complex

The ultramafic–alkaline–carbonatite complex Tiksheozero is located near the NE continental margin of the Karelian Craton within Archaean (2.74–2.72 Ga, e.g., Bibikova et al., 1997) tonalite–trondhjemite–granodiorite gneisses (Fig. 1a). The Neoarchaean junction zone between the Karelian and Kola provinces was a zone of particularly intense tectonic, magmatic and hydrothermal activity during or after the Palaeoproterozoic (1.94–1.75 Ga) Kola–Karelian orogeny (e.g., Bibikova et al., 2001). Age estimations of carbonatites are based on few K/Ar ages from biotites and amphiboles (2.0–1.8 Ga, Klyunin and Panichev, 1987) as well as a $^{207}Pb/^{206}Pb$ isochron of three apatites (1980±170 Ma, Shchiptsov et al., 1991). Therefore, the emplacement of the complex can be related to Palaeoproterozoic activity of the Neoarchaean junction zone. Bibikova et al. (2001) reported for all investigated rocks of the junction zone a complete reset of titanite ages to 1780–1750 Ma recording temperatures higher than 650 °C for this late Palaeoproterozoic overprint. Extensive hydrothermal activity is evidenced by abundant and newly grown titanite, and a small age difference between titanite and rutile ages (Bibikova et al., 2001).

The Tiksheozero carbonatite complex is a typical ring complexes where carbonatites are associated with intrusions of ultramafic and alkaline rocks. Klyunin and Panichev (1987) postulated five separate intrusion phases: (1) olivinites; (2) pyroxenites; (3) theralites, jacupirangites and ijolites; (4) nepheline syenites; and (5) carbonatites. Carbonatites occur as large bodies which are more than several hundred meters wide and up to 3 km long (Fig 1b). They were drilled to a depth of about 500 m (Fig. 1b, c). Mineral composition, grain size and rock colour vary considerably within these bodies. The main minerals of carbonatites (calcite, phlogopite, amphibole, apatite and magnetite) in places form layered structures but in other places silicate and oxide minerals form mixed clusters within a pure carbonatitic matrix.

Carbonatized silicic rocks are mainly pyroxenites or amphibolites containing between 10% and 50% carbonate minerals. In an earlier work (Tikhomirova et al., 1993) they were ascribed as carbonate–silicate metasomatites. The pyroxenites are located around carbonatite bodies (Fig. 1b, c) and are extensively altered in close contact to them. Alteration involves amphibolization, phlogopitization, apatitization and carbonatization in varying degrees. Amphibole or phlogopite may be replaced by late biotite. Carbonates (mainly calcite) form veinlets and clusters within such rocks. Local intense reworking is reported by strong foliation and granoblastic textures of some silicate and carbonatite rocks especially in their contact zones.

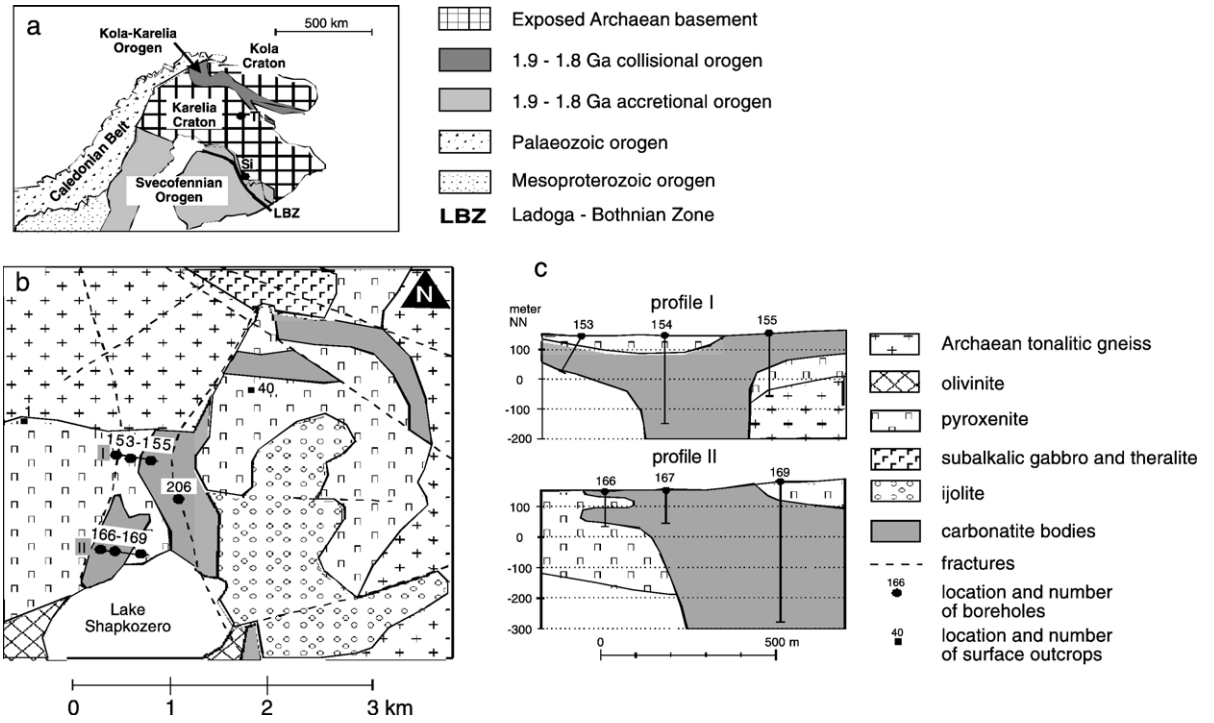

Fig. 1. (a) Major tectonic units of Fennoscandia after Zhao et al. (2002) and location of the Tiksheozero (Ti) and Siilinjärvi (Si) carbonatite complexes. (b) Simplified geological map of the Tiksheozero carbonatite complex after Tikhomirova et al. (1993) with selected borehole locations and sample locations at surface. (c) Schematic cross section through the Tiksheozero carbonatite body along profile I and II according to results from drill cores. Locations of the two profiles are given in (b). (Samples from borehole 169 are used for detailed mineral isotope investigation).

In 1995 we documented a large number of samples from boreholes drilled through large carbonatite bodies (Fig. 1b, c). Borehole 169 was the best documented at that time. Seven samples from borehole 169 (taken at different depths from 108 m to 391 m) and one sample from borehole 154 were chosen for a detailed geochemical and isotope study (O, C, Rb/Sr, Pb/Pb) using mineral separates of the rock-forming minerals (carbonate, apatite, phlogopite, amphibole, magnetite). 22 additional samples from boreholes and various carbonatized silicic rocks from surface outcrops were used for the characterization of the oxygen and carbon isotope composition of carbonates. Mineral separates from calcitic amphibolites, previously analyzed for their oxygen isotope composition (Tikhomirova et al., 1993), were analyzed here for Rb/Sr and Sm/Nd. A sample list and short sample descriptions are available in the Supplementary data in the Appendix.

2.2. Siilinjärvi carbonatite complex

The Siilinjärvi carbonatite complex is situated at the southern border of the Karelian Craton within Archaean (3.2–2.7 Ga, Hölttä et al., 2000) trondhjemitic–tonalitic–granodioritic/granitic gneisses along the Lake Ladoga–Central Bothnia deep fracture zone (Fig. 1a). The formation age of carbonatites was inferred from U/Pb investigations on zircons as 2.58±0.20 Ga (Patchett et al., 1981) and 2.605±0.006 Ga (cited as personal communication from Kuovo in Tilton and Bell, 1994). Scattering K/Ar ages (1.78–2.53 Ga, Puustinen, 1972) probably result from severe overprint related to the formation of the Svecofennian Orogen located to the south of the Karelian Craton representing a magmatic arc accretion (2.1–1.8 Ga, Zhao et al., 2002). The temperature of this thermal event is estimated as ≥500 °C according to reset of hornblende and biotite K/Ar ages to 1.85 and 1.80 Ga, respectively (Kontinen et al., 1992). Geothermobarometry studies indicate rather low pressures of about 5 kbar (Nironen, 1997).

The carbonatite complex forms a roughly tabular, north–south striking, sub-vertical body, about 16 km long and up to 1.5 km wide (Puustinen, 1971). The rocks comprise interlayered glimmerite (phlogopite rock), carbonatite and mixed rocks with varying contents of phlogopite, carbonate, apatite and amphibole. White carbonatite rocks may contain lenses of grey fine-grained carbonatite. The carbonate content

increases towards the centre of the sub-vertical carbonatite body. Syenitic rocks occur at both (west and east) margins towards the host granitic gneisses and were reinterpreted by a careful petrological and geochemical study as fenitized host rocks (Herms, 1986). Glimmerite formed earlier than carbonatite according to field relationships. It is considered either as a fenitized ultramafic phase (Puustinen, 1971) or as ultrafenitized host rocks (Herms, 1986). The intrusion of carbonatites occurred in several stages as induced from carbonatitic vein relationships.

10 samples representing different types of carbonatites and carbonatized phlogopite–amphibole rocks have been taken in the open pit of Siilinjärvi during a sampling campaign in 1993. The macroscopic description of the samples is available in the Supplementary data in the Appendix. Rock-forming minerals (carbonate of different colour, apatite, phlogopite, amphibole) have been separated from all 10 samples for isotope analyses (O, C, Rb/Sr, Sm/Nd, Pb/Pb).

3. Analytical methods

Thin sections were analysed in addition to conventional microscopy by a cathodoluminescence (CL) microscope HC1–LM equipped with a hot cathode electron gun (Neuser et al., 1995). The system was operated at 14 kV accelerating voltage and a current density of about 10 mA/mm^2. Documentation of the CL behaviour was realised by an attached Nicon camera and Kodak Ektachrome 400 material.

Isotope analyses were performed at three Isotope Laboratories: the Isotope Laboratory of the TU Bergakademie Freiberg ($\delta^{13}C$, $\delta^{18}O$, Rb/Sr), the Institute of Precambrian Geology and Geochronology (IPGG) in St. Petersburg (Rb/Sr, Sm/Nd, U/Pb, Pb/Pb), and the Max-Planck-Institute (MPI) at Mainz (Pb/Pb).

The oxygen isotope composition of silicate minerals, apatite, magnetite and whole rocks was determined according to the procedure of Borthwick and Harmon (1982) using ClF_3 as oxidizing agent. All analyses were performed twice and the reproducibility is <0.2‰. Measurements have been corrected based on analyses of the standard NBS 28 (accepted value=9.6‰). The carbon and oxygen isotope composition of carbonates was determined according to the procedure of McCrea (1950). We used the method of chemical separation in order to obtain the isotope composition for both calcite and dolomite contained in our separated carbonate minerals (compare Section 4.1) of one sample (e.g., Ray and Ramesh, 1998). We applied the three-step procedure of Walters et al. (1972) in accordance with our average carbonate grain size. This procedure involves CO_2 extraction from calcite after 1-h reaction, an in-between pumping stage to reject CO_2 from calcite–dolomite mixtures (1–3 h) and finally CO_2 extraction from dolomite (3–72 h). Isotope measurements were carried out on a Delta E mass spectrometer. Reproducibility of analyses is better than ±0.2‰.

Rb, Sr, Sm, Nd, U, and Pb concentrations were determined by isotope dilution. Precision is estimated at about 1%. Isotope measurements were carried out on Finnigan MAT 262 (Rb, Sr, Pb at the Freiberg Laboratory), and Finnigan MAT 261 (Rb, Sr, Sm, Nd, U, Pb at the IPGG) mass spectrometers under static multi-collector mode. During the course of this study the NBS 987 standard yielded $^{87}Sr/^{86}Sr=0.71033\pm5$ (2σ, $n=18$) at the Freiberg Laboratory and $^{87}Sr/^{86}Sr=0.71025\pm2$ (2σ, $n=10$) at the St. Petersburg Institute. All Sr isotope data have been corrected to the accepted NBS 987 value of 0.71025. The $^{143}Nd/^{144}Nd$ ratio was normalized within-run to $^{148}Nd/^{144}Nd=0.241570$ and then adjusted to a $^{143}Nd/^{144}Nd$ value of 0.511860 for La Jolla. The La Jolla standard yielded $^{143}Nd/^{144}Nd=0.511852\pm4$ (2σ, $n=10$). Assigned errors (2σ) for $^{147}Sm/^{144}Nd$ and $^{143}Nd/^{144}Nd$ were ±0.3% and ±0.000015, $^{87}Rb/^{86}Sr$ ±0.5%, $^{87}Sr/^{86}Sr$ ±0.000025 according to results of multiple analyses of standard (external reproducibility). The blank level for Sm was 0.01 ng and 0.05 ng for Nd, 0.05 ng for Rb and 0.2 ng for Sr.

The Pb isotope composition and the Pb and U concentrations were determined in different aliquots of each sample (50–100 mg) by isotope dilution techniques with the use of a mixed $^{208}Pb/^{235}U$ tracer (IPGG, St. Petersburg). The methods of chemical decomposition and Pb and U extraction were analogous to those described in Manhes et al. (1978). Pb and U from whole rock samples and mineral fractions were separated by anion exchange in HBr media. Total blank levels during analytical work did not exceed 0.05 ng for Pb and 0.005 ng for U. Isotope analysis of lead was carried out with the aid of silicate emitter. The mass-discrimination of 0.0013 ± 0.0003 amu^{-1}, determined by numerous measurements of NBS 982, was used to correct for fractionation in the samples. Average values for NBS 982 measured during the course of these analyses are $^{206}Pb/^{204}Pb=36.643$, $^{207}Pb/^{204}Pb=17.092$, $^{208}Pb/^{204}Pb=36.551$. Estimated errors based on between-run precision of the standard are ±0.03% amu^{-1}, within-run precision for individual Pb analyses was ±0.006–0.008%. The raw U/Pb data were processed with the PBDAT computer program. Data for BCR-1 standard (mean of 8 runs) were: $^{206}Pb/^{204}Pb=18.815$,

$^{207}Pb/^{204}Pb = 15.638$, $^{208}Pb/^{204}Pb = 38.732$, Pb = 13.396 ppm, U = 1.703 ppm.

4. Results

4.1. Microscopic investigations of thin sections

4.1.1. Tiksheozero carbonatite complex

Carbonatite rocks from the large carbonatite bodies are usually medium-grained and often form an idiomorphic to hypidiomorphic texture. In most samples the carbonate content varies from 80% to 90%. Apatite is mostly equally distributed within the carbonate matrix and occurs mainly as round, elongated grains (Fig. 2c).

The application of cathodoluminescence microscopy on our carbonatites was essential to distinguish different carbonate generations (Fig. 2b, d). Early calcitic carbonate forms medium grained textures with triple junctions indicating equilibrium conditions under subsolidus conditions (cc-1, Fig. 2a, b). Alteration of these calcite grains occurs mainly along grain borders leading to a change in the CL colour from reddish-brown to orange or even yellow without formation of new crystals or crystal borders (cc-2 in Fig. 2c, d). However, the calcite twinning structure may be disturbed at the rim of these grains. These calcite alteration zones are recognizable in thin sections by darker "dirty" regions caused by lots of minute fluid inclusions (Fig. 2c). Adjacent apatite shows a change of the CL colour from violet to blue along borders and fractures (Fig. 2d). Comparison of thin sections and corresponding hand specimens show that alteration processes and formation of cc-2 lead to a change in colour from pinkish to grey. Therefore, primary carbonatites without alteration can usually be recognized by their pinkish colour.

We used the brown to black CL colour for distinguishing dolomitic from calcitic carbonates supported on a few thin sections by EDX analyses (e.g., Fig. 2d). Accordingly, the dolomite content is minor (about 5–10%) in all borehole samples from large carbonatite bodies. Dolomite grains are usually equally distributed within the calcite matrix and may be located within calcite triple junctions. Therefore, all carbonate separates constitute a mix of major calcite and minor dolomite. The most abundant carbonate variety is cc-1 altered in various degrees to cc-2.

4.1.2. Siilinjärvi carbonatite complex

In difference to Tiksheozero, both calcitic and dolomitic carbonatites are present. Dark grey fine-grained dolomite carbonatites (beforsites) occur as lenses within white or pink medium-grained calcitic carbonatites (alvikites). Therefore, beforsites can be regarded as the earliest carbonatite phase. They contain large corroded apatite crystals and a few large dolomite phenocrysts. Carbonates in the alvikites often form an idiomorphic texture with triple junctions (cc-2 in Fig. 2e, g). Larger porphyric grains of calcite or dolomite are observed within the medium-grained carbonate matrix (Fig. 2g). Carbonatites usually have carbonate concentrations higher than 70%. Apatite was found in all carbonatites as rounded grains. Further non-carbonate minerals are phlogopite (tetraferriphlogopite) and rare amphibole (richterite) mainly as silicate layers or clusters within carbonatites.

Rock-forming minerals of glimmerites are phlogopite and amphibole (richterite) with minor carbonate (<50 vol.%), apatite and accessory zircon. Minerals reach very large grain sizes up to 10 cm in some of the glimmerite–richterite rocks. Deformation of these rocks becomes evident from deformed and broken crystals of phlogopite, amphibole and zircon.

According to conventional and CL spectroscopy, several generations of carbonates can be distinguished. Large porphyric calcite and dolomite grains (cc-1, do-1) seem to be an early generation because they are commonly replaced by medium-grained calcite (cc-2, Fig. 2g, h) and/or fine-grained calcite–dolomite veinlets (cc-do-3). The latest generation of carbonates (cc-do-3) forms fine-grained clusters in triple junctions and/or along grain boundaries and can replace the idiomorphic carbonate matrix (cc-2) and/or early dolomitic grains. Such carbonates can clearly be identified by their yellow CL colour (Fig. 2f, h). Adjacent apatite crystals show a change of their CL colour from purple to blue. All separated carbonates represent mixtures of major calcite and minor dolomite.

4.2. O and C isotope composition

4.2.1. Tiksheozero carbonatite complex

Tiksheozero carbonate mineral separates from carbonatite bodies sampled in boreholes generally display a very uniform carbon and oxygen isotope composition at constant reaction times (for all but one separate with calcite reaction time from −5.2 to −4.9‰ and from 6.8 to 7.3‰, respectively). However, the $\delta^{18}O$ values are significantly higher, when dolomite reaction time was applied (field D in Fig. 3a, for all but three separates from 9.1 to 9.5‰).

Whole rock samples with calcite reaction time display a more heterogeneous oxygen isotope composition (from 6.7 to 8.9‰) compared to the carbonate

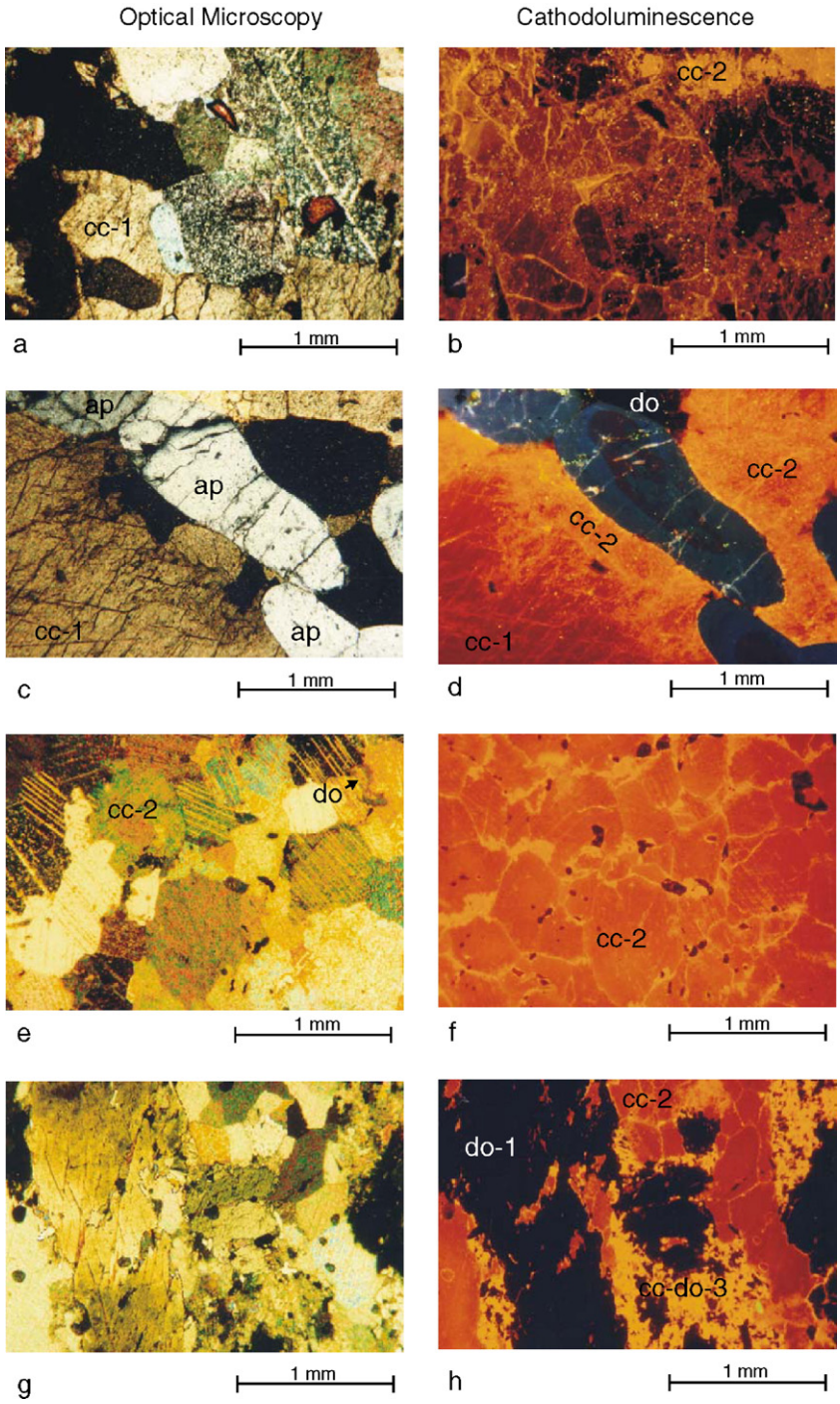

Fig. 2. Optical (a, c, e, g) and corresponding cathodoluminescence (b, d, f, h) microscopy of thin sections from Tiksheozero (a–d) and Siilinjärvi (e–h) carbonatites. ap – apatite, cc – calcite, do – dolomite. Compare text for discussion.

separates where the $\delta^{18}O$ signature is often shifted towards higher values (trend A in Fig. 3a), although equal values were obtained in some cases. There is no difference in the carbon isotope composition between carbonate separates and whole rocks (Fig. 3a). When differently coloured pieces of the same rock are compared, the grey carbonatite yields elevated $\delta^{18}O$ values in comparison to slightly pinkish parts.

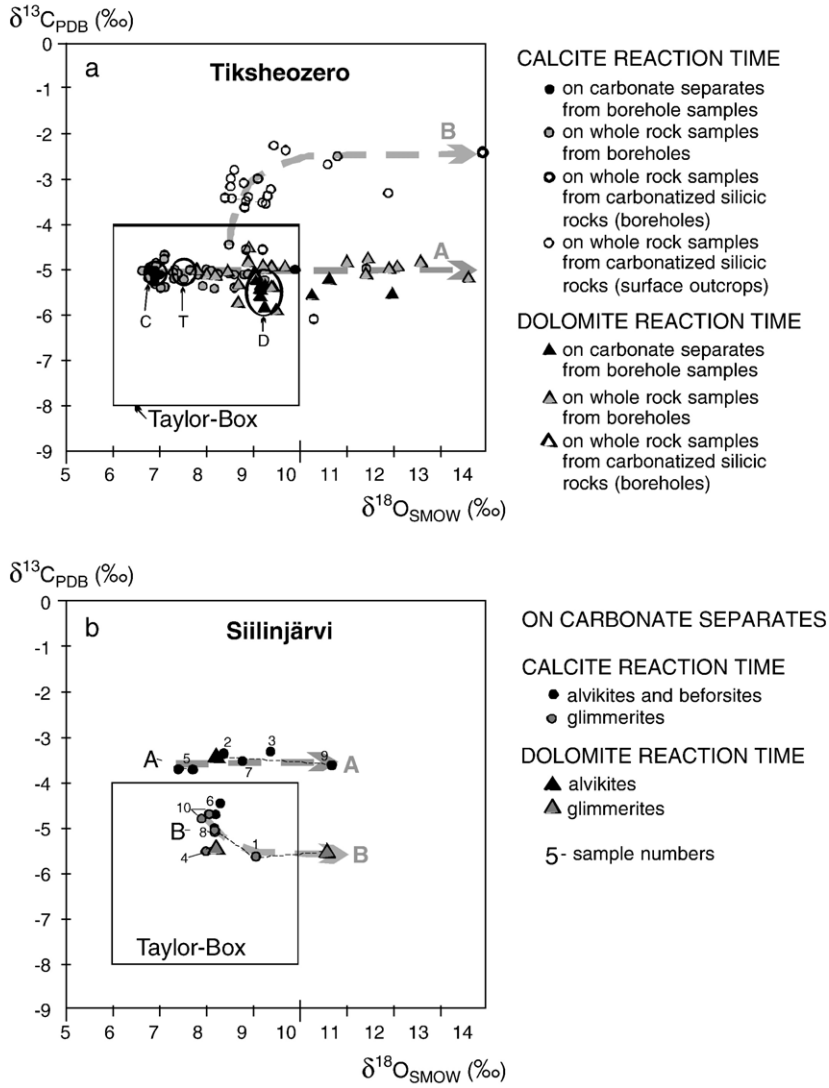

Fig. 3. Carbon and oxygen isotope composition of carbonates from Tiksheozero (a) and Siilinjärvi (b). Analytical errors are smaller than symbols. For Tiksheozero data are given for separated carbonates and whole rock samples with different reaction times (chemical separation, see section analytical methods). Field C – carbonate separates from borehole samples with calcite reaction time, field D – carbonate separates from borehole samples with dolomite reaction time without three outliers, field T – primary isotope composition according to Tikhomirova et al. (1993). For Siilinjärvi only data for separated carbonates are given. Taylor box is the field of "primary igneous carbonatites" according to Taylor et al. (1967). Compare text for discussion of various fields and trends A and B.

Carbonates from carbonatized silicic rocks define a second trend (Fig. 3a, trend B). These carbonates display not only increased oxygen, but clearly higher carbon isotope values (from 8.4 to 11.9‰ and from −4.6 to −2.2‰, respectively).

The calculated oxygen isotope temperatures (Table 1) yield a similar range for calcite – amphibole (490–600 °C), and calcite – magnetite pairs (490–580 °C). The apatite oxygen isotope composition is also quite homogeneous (4.2 to 4.7‰). Temperatures, calculated for calcite – apatite pairs give slightly higher values of 560–750 °C. The oxygen isotope composition of mica leads to lower isotope temperatures for calcite – phlogopite pairs (380–440 °C according to Bottinga and Javoy, 1975; 270–330 °C according to Fortier and Lüttge, 1995). Red calcite from sample 169-79 results in lower isotope temperatures than white carbonate of this sample.

4.2.2. Siilinjärvi carbonatite complex

Differently coloured carbonates of one sample often show quite distinct oxygen and carbon isotope

Table 1
Oxygen isotope composition ($\delta^{18}O$ vs. VSMOW in ‰) of carbonate and silicate mineral fractions and calculated isotope temperatures (T in °C) for the Tiksheozero and Siilinjärvi carbonatite complexes

Sample	$\delta^{18}O$	$\delta^{18}O$	$\delta^{18}O$	$\delta^{18}O$	$\delta^{18}O$	T_{Cc-Am} (°C)	T_{Cc-Ap} (°C)	T_{Cc-Phl} (°C)		T_{Cc-Mgt} (°C)
	Cc	Am	Ap	Phl	Mgt	1	2	3	4	5
Tiksheozero										
169-34	6.9	4.4	4.2	–	−1.5	560	620	–	–	570
169-53	6.9	4.3	4.7	1.7	−2.5	550	750	300	410	520
169-55	6.9	4.3	4.3	1.1	−2.6	550	640	270	380	520
169-67	6.8	4.3	4.4	2.2	−1.8	560	690	330	440	560
169-79(r)	9.9	4.3	4.4	2.1	−2.3	340	300	200	300	420
169-79(w)	7.0					540	640	310	420	520
169-81	7.3	4.1	4.3	1.7 (gm)	−2.8	490	560	280	390	490
				2.2 (ph)		–	–	300	410	–
169-89	6.9	4.3	4.3	2.2	−2.6	600	750	330	440	520
154-23	6.9	4.1	4.4	1.7	−1.3	530	660	300	410	580
Siilinjärvi										
1(r)	8.2	–	5.7	4.4	–	–	560	390	490	–
1(o)	8.2	–	–	–	–	–	–			–
1(w)	9.1	–	–	–	–	–	–			–
2	8.4	–	4.5	3.2	–	450	430	300	410	–
3	9.4	4.7	4.7	4.4	–	–	360	310	420	–
4	8.0	–	4.9	4.5	–	500	540	410	520	–
5(r)	7.7	4.9	5.4	3.6	–	600	720	–	–	–
5(w)	7.4	5.5	–	–	–	–	–	360	470	–
6	8.2	5.2	5.1	4.5	–	510	540	390	500	–
7	8.8	–	4.4	4.0	–	–	380	320	430	–
8	8.2	5.5	4.5	4.0	–	540	290	360	470	–
9	10.7	5.5	4.9	4.1	–	360	290	240	350	–
10	8.0	5.0	4.9	4.6	–	520	540	420	530	–

Cc – calcite, Am – amphibole, Ap – apatite, Phl – phlogopite, Mgt – magnetite. (ph) – phenocryst, (gm) – groundmass. (r) – compared to red-coloured carbonate separate, (o) – compared to orange-coloured carbonate separate, (w) – compared to white-coloured carbonate separate. Temperature calculations 1 and 4 – according to Bottinga and Javoy (1975), 2 – according to Fortier and Lüttge (1995), 3 – according to Fortier et al. (1994), 5 – according to Chiba et al. (1989) and Cole et al. (2004).

compositions (see Table 1). Carbonates from alvikites and beforsites have higher $\delta^{13}C$ values (from −3.7 to −3.3‰) compared to those from glimmerites (Fig. 3b) with exception of sample 6 (two carbonate separates were analysed from this sample) which contains lenses of glimmerites and therefore can be regarded as a mixed sample. Alvikites and beforsites have a homogeneous carbon, but variable oxygen isotope composition resembling the pattern of Tiksheozero carbonates from large carbonatite bodies (Fig. 3b, trend A).

Larger variations and sometimes lower values are obtained for calculated oxygen isotope temperatures for carbonate–silicate (360–600 °C), and carbonate–phosphate (290–720 °C) mineral pairs compared to Tiksheozero samples (Table 1). The sample with the lowest oxygen isotope value of the carbonate (sample 5) gives the highest temperature (cc-amph: 600 °C; cc-ap: 720 °C) similar to that for Tiksheozero.

4.3. Sr isotope composition

4.3.1. Tiksheozero carbonatite complex

Rb/Sr analyses of whole rocks and their minerals have been determined on eight samples of carbonatites from boreholes (Table 2a) and five additional samples of carbonatized silicic rocks sampled at surface outcrops (Table 2b). Mineral separates and corresponding whole rocks define isochrons with ages between 1700–1800 Ma; the ages are mainly controlled by the Rb/Sr system of the micas (Table 2a). Isochrons are not well defined since not all minerals lie on the deduced line indicating the opening of the Rb/Sr system. Two phlogopite concentrates were separated from sample 169-81 resulting in different isochron ages (Table 2a; Fig. 4: 1698±27 Ma and 1906±30 Ma) with a higher age obtained from larger phenocryst grains. Four of the nine analysed mica concentrates give an Rb/Sr isochron age of 1684±35 Ma (MSWD=0.72). When measured $^{87}Sr/^{86}Sr$ ratios are recalculated to initial ones at the time

Table 2a
Rb–Sr isotope data on whole rock samples and mineral separates from the Tiksheozero carbonatite complex (borehole samples)

Sample, mineral	Rb (ppm)	Sr (ppm)	$^{87}Rb/^{86}Sr$	$^{87}Sr/^{86}Sr$ measured[a]	$^{87}Sr/^{86}Sr$ (1.98 Ga)	ε_{Sr} (1.98 Ga)	Rb/Sr-isochron age (Ma)[b]	$(^{87}Sr/^{86}Sr)_i$ from isochron
169-34, Cc	–	6336	0	0.70249	0.70249	5.0	–	–
169-34, Ap	–	4711	0	0.70248	0.70248	4.8		
169-34, Am	2.42	135	0.05187	0.7043	0.70283			
169-53, Cc	0.16	4953	0.00010	0.70247	0.70247	4.6		
169-53, Ap	1.16	3696	0.00091	0.70240	0.70237	3.3		
169-53, Am	0.93	51.5	0.05228	0.70389	0.70240			
169-53, Phl	376	15.6	83.98	2.81943	(0.42474)		1754±37	0.70247
169-55, Cc	–	5436	0	0.70270	0.70270	7.9		
169-55, Ap	–	5092	0	0.70268	0.70268	7.7		
169-55, Am	0.96	57.0	0.04881	0.70369	0.70230			
169-55, Phl	391	20.7	62.977	2.28671	(0.49092)		1749±37	0.70261
169-67, WR	6.22	4718	0.00381	0.70248	0.70237			
169-67, Cc	–	5562	0	0.70242	0.70242	4.0		
169-67, Ap	–	4224	0	0.70228	0.70228	2.0		
169-67, Am	0.68	54.0	0.03659	0.70322	0.70218			
169-67, Phl	379	8.22	201.21	5.90324	(0.16574)		1797±28	0.70234
169-79, WR	4.52	3577	0.00365	0.70258	0.70248			
169-79, Cc(r)	–	3584	0	0.70252	0.70252	5.4		
169-79, Ap	5.40	4135	0.00378	0.70240	0.70229	2.1		
169-79, Am	0.41	32.0	0.03740	0.70323	0.70216			
169-79, Phl	245	4.34	255.49	6.44172	(<0)		1564±25	0.70243
169-81, WR	13.9	3289	0.01223	0.70245	0.70210			
169-81, Cc	–	5035	0	0.70244	0.70244	4.2		
169-81, Ap	2.16	4036	0.00155	0.70257	0.70253	5.5		
169-81, Am	0.49	35.49	0.03979	0.70351	0.70237			
169-81, Phl-1	293	6.50	189.38	5.32327	(<0)		1698±27	0.70242
169-81, Phl-2	313	19.42	53.43	2.16834	(<0)		1906±30	0.70238
169-89, WR	44.4	3560	0.03610	0.70289	0.70186			
169-89, Cc	–	4921	0	0.70250	0.70250	5.1		
169-89, Ap	2.85	3876	0.00213	0.70249	0.70243	4.1		
169-89, Phl	278	5.14	250.05	6.83657	(<0)		1707±36	0.70231
154-123, WR	30.4	4280	0.02054	0.70298	0.70239			
154-123, Cc	0.07	5677	0.00004	0.70243	0.70243	4.1		
154-123, Ap	–	3822	0	0.70236	0.70236	3.1		
154-123, Phl	471	9.33	231.26	6.68589	(0.09151)		1799±38	0.70241

– not determined.

[a] The 2σ error is always <0.00001 for all calcites and albite, <0.00005 for all apatites and biotite, <0.00008 for all whole rocks and amphiboles, and <0.00023 for all phlogopites.

[b] Rb/Sr isochron ages of samples were calculated using available whole rock and mineral data of the respective samples, except for sample 169-81, where two isochrones using different phlogopite separates were calculated. Isochron ages are mainly controlled by phlogopite and are given for whole rock together with their corresponding mineral separates on the same line as the used phlogopite separate. Sample 169-81: Phl-2 are large-grained phenocrystic grains.

of carbonatite formation (t=1980 Ma according to Shchiptsov et al., 1991 and unpublished data from own zircon dating – Tichomirowa et al., in preparation) most phlogopite separates give too low unrealistic initial values (lower than 0.7, given in parenthesis in Tables 2a and 2b) whereas the initial Sr ratios calculated from isochrons generally agree with those of their calcites and apatites.

We used pure mineral separates of calcite and apatite for derivation of the initial $^{87}Sr/^{86}Sr$ isotope composition. Calculated initial $^{87}Sr/^{86}Sr$ ratios are significantly lower and more consistent for calcites and apatites from carbonatite borehole samples (for all but one sample from 0.70228 to 0.70253) compared to those from carbonatized silicic surface samples (from 0.70273 to 0.70378). Although some of the calculated initial Sr isotope ratios for whole rocks agree well with those from calcites and apatites, they generally show a larger scatter with both higher and lower values.

The variation of the Sr isotope composition of calcites and apatites from borehole samples is significantly greater than analytical reproducibility. Coexisting calcite

Table 2b
Rb–Sr and Sm–Nd isotope data on whole rock samples and mineral separates from the Tiksheozero carbonatite complex (carbonatized silicic rocks)

Sample, mineral	Rb (ppm)	Sr (ppm)	$^{87}Rb/^{86}Sr$	$^{87}Sr/^{86}Sr$ measured [a]	$^{87}Sr/^{86}Sr$ (1.98 Ga)	ε_{Sr} (1.98 Ga)	Sm (ppm)	Nd (ppm)	$^{147}Sm/^{144}Nd$	$^{143}Nd/^{144}Nd$ measured [b]	$^{143}Nd/^{144}Nd$ (1.98 Ga)	ε_{Nd} (1.98 Ga)
1-4-1, WR	31.0	2851	0.03143	0.70446	0.70360		18.1	124.2	0.08831	0.51132	0.51017	1.9
1-4-1, Cc	0.20	8174	0.00007	0.70301	0.70301	12.3	7.19	24.0	0.18103	0.51243	0.51007	0
1-4-1, Ap	0.58	9340	0.00018	0.70280	0.70279	9.3	98.3	844	0.07038	0.51161	0.51069	12.2
1-4-1, Am	1.14	203	0.01614	0.70329	0.70283		4.96	14.8	0.20287	0.51259	0.50995	−2.4
1-4-1, Bt	195	41.1	14.22	1.06490	(0.65942)		0.39	3.02	0.07899	0.51120	0.51017	1.9
1-4-1, Ab	1.15	206	0.01606	0.70488	0.70442		1.56	14.5	0.06526	0.51115	0.51030	4.4
1-4-2, WR	21.6	3344	0.01870	0.70362	0.70308		4.77	17.5	0.16464	0.51232	0.51017	1.9
1-4-2, Cc	0.28	5067	0.00016	0.70334	0.70333	17.0	3.72	9.66	0.23260	0.51294	0.50991	−3.2
40-1-4, WR	0.32	219	0.00422	0.70393	0.70381		2.25	9.44	0.14421	0.51194	0.51006	−0.2
40-1-4, Cc	0.59	1391	0.00122	0.70382	0.70378	23.4	2.83	14.7	0.11624	0.51161	0.51009	0.4
40-1-4, Am	0.40	60.9	0.01906	0.70413	0.7359		2.40	9.27	0.15635	0.51211	0.51007	0
40-1-7, WR	2.78	162	0.04974	0.70482	0.70340		2.05	8.43	0.14672	0.51201	0.51010	0.5
40-1-7, Cc	0.17	891	0.00055	0.70372	0.70370	22.2	0.98	6.53	0.09091	0.51134	0.51015	1.6
40-1-7, Am	2.70	110	0.07117	0.70440	0.70237		2.74	11.4	0.14539	0.51197	0.51007	0
T1, WR	13.7	2095	0.01824	0.70324	0.70272		9.81	78.41	0.07563	0.51118	0.51019	2.3
T1, Cc	0.38	3548	0.00031	0.70274	0.70273	8.4	3.89	27.43	0.08584	0.51120	0.51008	0.2
T1, Am	6.68	53.2	0.36335	0.70445	0.69409		0.38	3.15	0.07353	0.51109	0.51013	1.2
T1, Ab	2.42	70.8	0.09890	0.70503	0.70221		0.65	6.11	0.06464	0.51100	0.51016	1.7

[a] The 2σ error is always <0.00004.
[b] The 2σ error is always <0.00007.

and apatite from the same sample are only in two cases identical within error (Fig. 5). In most samples calcite has a slightly higher initial Sr ratio accompanied by a higher Sr concentration compared to the corresponding apatite. The largest difference between apatite and calcite is found in sample 169-79 with the red calcite having a lower Sr concentration and a significantly higher Sr isotope ratio compared to the coexisting apatite.

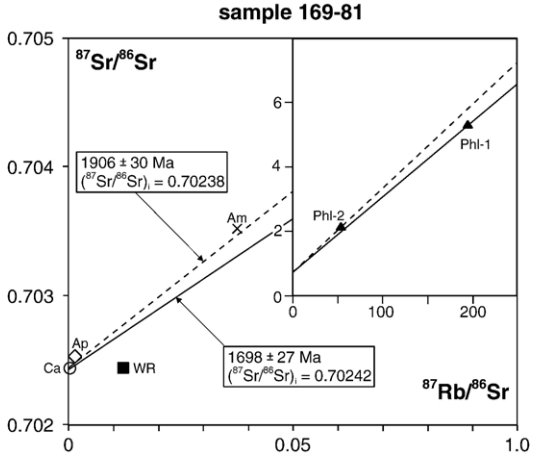

Fig. 4. Rb–Sr isochron diagram for sample 169-81 from Tiksheozero. Two isochrons are calculated according to two separated phlogopite concentrates. Phl-1 is a separate from larger grained phenocryst micas, Phl-2 is a separate from fine-grained micas of the groundmass.

4.3.2. Siilinjärvi carbonatite complex

Rb/Sr analyses have been obtained for eight whole rock samples and their mineral separates (Table 3). The resulting isochrons give ages between 1754 and 2031 Ma. Four of the seven analyzed phlogopite separates define a Rb/Sr isochron with an age of 1768±16 Ma (MSWD=0.143; $^{87}Sr/^{86}Sr_i$= 0.6958).

The initial Sr isotope composition of calcites and apatites show a much larger variation (from 0.70149 to 0.70652) compared to those from the Tiksheozero complex (Table 3; Fig. 5). Larger Sr isotope differences are also observed for corresponding calcites and apatites and between differently coloured calcites from the same sample (e.g., sample 6: white calcite – 0.70556, red calcite – 0.70359). Apatites and calcites from glimmerites have a higher Sr initial ratio compared to those from alvikites (Fig. 5: from 0.70518 to 0.70652 and from 0.70149 to 0.70416, respectively – if sample 6 is not taken into consideration because of its intermediate composition, compare Section 4.2.2).

4.4. Nd isotope composition

4.4.1. Tiksheozero carbonatite complex

Available Nd data characterized only surface outcrop samples from carbonatized amphibolites (Table 2b). Whole rock and corresponding mineral separates give errorchrons with ages ranging between 1700 and

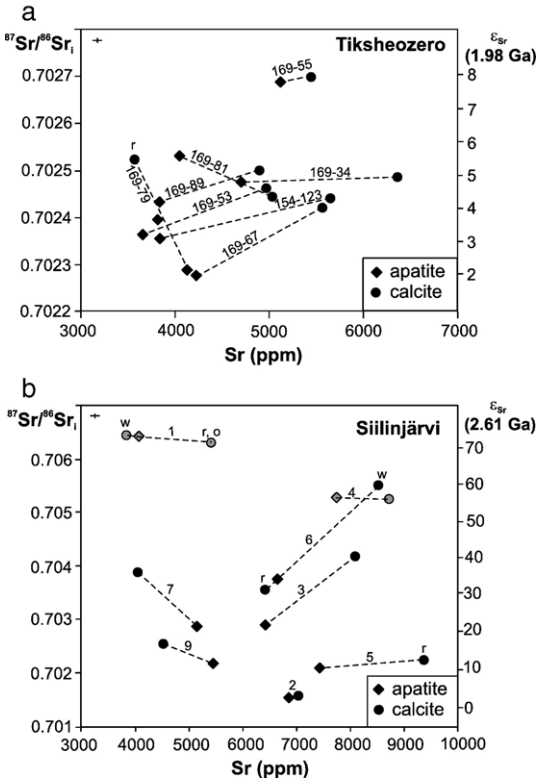

Fig. 5. Sr concentration versus initial Sr isotope ratios for separated apatites and calcites from borehole samples of the Tiksheozero complex (a) and from outcrop samples of the Siilinjärvi carbonatite complex (b). Error bars are given in the upper left corner. Tie lines joint apatite – calcite data from the same sample with indicated sample numbers. r, o, w – indicate colour of carbonates (red, orange, white). In (b) alvikites are shown as black symbols, glimmerites as grey symbols.

1900 Ma. The only apatite separate analyzed (sample 1-4-1) does not fit the errorchron but plots well above this regression line. If all five whole rocks are plotted together they yield a Sm/Nd errorchron with a slope corresponding to an age of 1855±330 Ma, whereas three of these whole rock samples define a Sm/Nd isochron with an age very similar to the formation age of the carbonatite (samples 1-4-1, 1-4-2 and T 1: 1951± 110 Ma, MSWD=1.3, ε_{Nd}=+1.8). Calculated epsilon values show large variations for different minerals of the same sample (up to 14 epsilon values). The lowest variations show whole rock samples (−0.2 and +2.3, Fig. 6).

4.4.2. Siilinjärvi carbonatite complex

Three samples (whole rock and mineral separates) were analyzed from the Siilinjärvi carbonatite complex (Table 3). No isochron could be derived mainly because of the very low difference in $^{147}Sm/^{144}Nd$ ratios. If the amphibole and calcite from sample 2 are excluded (which obviously show distortion of their Sm/Nd system, compare Fig. 6), an errorchron age of 3.3± 0.9 Ga is obtained for all remaining mineral separates and whole rocks. If only apatites and whole rocks (which both have the highest Nd concentrations) from all three samples are plotted together, a Sm/Nd errorchron is obtained with a slope corresponding to an age of 2.7±2.0 Ga (MSWD=4.8, ε_{Nd}=+3.2), which is similar to the carbonatite formation age. The large age error mainly results from the low spread in $^{147}Sm/^{144}Nd$ ratios, whereas the high MSWD is caused by some deviation of the apatites from sample 6 and 7 from the regression line. The calculated epsilon values of minerals scatter (e.g., for carbonate from −5.5 to +2.5) while whole rock samples display more homogeneous epsilon values (between +1.2 and +2.4) which are mainly consistent with those of apatites (from +0.7 to +3.4; Fig. 6).

4.5. Pb isotope composition

4.5.1. Tiksheozero carbonatite complex

U–Pb isotope data have been obtained for apatite separates from borehole samples of large carbonatite bodies and for whole rocks from surface samples of carbonatized amphibolites. These are available in the Supplementary data in the Appendix. Both data sets yield secondary isochrons with ages of about 1800–1900 Ma (Fig. 7a). It is not possible to calculate initial Pb isotope ratios for most of the apatites since they have too high contents of radiogenic Pb so that decay corrections yield erratic initial ratios. Therefore, initial ratios were calculated for samples when correction for radiogenic Pb does not exceed 4% of the observed ratios (compare Kwon et al., 1989). No U concentrations were obtained for whole rocks so that in situ decay correction could not be applied. The lowest uncorrected $^{206}Pb/^{204}Pb$ (14.5–15.2) and $^{207}Pb/^{204}Pb$ (14.9–15.1) values are from whole rocks almost completely consisting of carbonate which probably have very low U contents so that correction for radiogenic lead is considered to be insignificant.

4.5.2. Siilinjärvi carbonatite complex

U/Pb results have been analysed for apatite from all ten samples and for further rock-forming minerals from samples 2, 6, 7 (available in the Supplementary data in the Appendix). These three samples yield secondary isochrons with ages between 1700 and 2000 Ma which are mainly determined by apatites having a high contribution of radiogenic Pb. Initial Pb ratios were calculated for samples when correction for

Table 3
Rb–Sr and Sm–Nd isotope data on whole rock samples and mineral separates from the Siilinjärvi carbonatite complex

Sample, mineral	Rb (ppm)	Sr (ppm)	$^{87}Rb/^{86}Sr$	$^{87}Sr/^{86}Sr$ measured[a]	$^{87}Sr/^{86}Sr$ (2.61 Ga)	ε_{Sr} (2.61 Ga)	Sm (ppm)	Nd (ppm)	$^{147}Sm/^{144}Nd$	$^{143}Nd/^{144}Nd$ measured[b]	$^{143}Nd/^{144}Nd$ (2.61 Ga)	ε_{Nd} (2.61 Ga)
1, WR	104	2680	0.11272	0.70912	0.70486							
1a, WR	78	154	1.46894	0.75012	0.69466							
1b, WR	16.6	4572	0.01050	0.70631	0.70591							
1, Cc(w)	0.40	3898	0.00030	0.70654	0.70652	73.4						
1, Cc(o)	–	5402	0	0.70638	0.70638	71.3						
1, Cc(r)	–	5421	0	0.70638	0.70638	71.3						
1, Ap	3.32	4052	0.00237	0.70666	0.70657	72.7						
1, Phl	287	13.6	72.145	2.52594	(<0)							
2, WR	50.5	6211	0.02353	0.70239	0.70150		22.3	147	0.09188	0.51095	0.50937	2.4
2, Cc	0.07	7035	0.00003	0.70157	0.70157	2.7	22.4	100	0.13545	0.51130	0.50897	−5.5
2, Ap	0.09	6923	0.00003	0.70149	0.70149	1.6	153	1075	0.08655	0.51081	0.50932	1.3
2, Am	22.2	141	0.45712	0.70482	(0.68756)		1.10	13.1	0.05097	0.51077	0.50990	12.7
2, Phl	470	54.4	26.779	1.45153	(0.44043)							
3, Cc	–	8052	0	0.70416	0.70416	39.7						
3, Ap	–	6456	0	0.70294	0.70294	22.3						
3, Phl	311	8.58	141.713	4.29823	(<0)							
4, WR	34.4	2223	0.04474	0.70652	0.70483							
4, Cc	–	8630	0	0.70518	0.70518	54.2						
4, Ap	–	7778	0	0.70525	0.70525	55.2						
4, Am	8.45	293	0.08328	0.70617	0.70302							
4, Phl	238	18.1	42.057	1.76620	(0.17824)							
5, WR	2.53	8200	0.00089	0.70173	0.70169							
5a, WR	0.78	8842	0.00026	0.70138	0.70137							
5b, WR	2.99	8827	0.00098	0.70188	0.70184							
5, Cc(r)	–	9387	0	0.70220	0.70220	11.8						
5, Ap	–	7455	0	0.70211	0.70211	10.4						
6, WR	15.6	8069	0.00558	0.70443	0.70422		11.3	68.4	0.10027	0.51106	0.50933	1.5
6, Cc(w)	0.08	8527	0.00003	0.70556	0.70556	59.6	9.96	70.2	0.08595	0.51068	0.50920	−1.0
6, Cc(r)	0.09	6472	0.00004	0.70359	0.70359	31.5	10.1	71.9	0.08504	0.51079	0.50929	0.7
6, Ap	0.15	6716	0.00007	0.70380	0.70380	34.5	163	1130	0.08735	0.51124	0.50949	4.7
6, Am	5.10	339	0.04343	0.70438	0.70274		0.71	4.23	0.10183	0.51044	0.50915	−2.0
6, Phl	385	33.5	36.743	1.77947	(0.39215)		0.04	0.29	0.07505	0.51092	0.50931	1.2
7, WR	82.3	2394	0.09946	0.70658	0.70283		38.0	246	0.09346	0.51098	0.50938	2.5
7, Do	1.61	4052	0.00115	0.70396	0.70392	35.6	8.71	57.0	0.09269	0.51096	0.50942	3.4
7, Ap	0.18	5132	0.00010	0.70281	0.70281	20.4	177	1199	0.08933	0.51072	0.50934	1.7
7, Phl	435	8.29	256.65	7.76987	(<0)		0.05	0.38	0.08051			
9, WR	26.0	4030	0.01866	0.70264	0.70194							
9a, WR	167	2146	0.22559	0.70899	0.70047							
9b, WR	1.88	5125	0.00106	0.70183	0.70179							
9, Cc	–	4511	0	0.70258	0.70258	17.1						
9, Ap	–	5452	0	0.70215	0.70215	11.0						
9, Phl	337	5.79	290.467	8.08843	(<0)							

– not determined.
[a] The 2σ error is always <0.00003 for all carbonates, <0.00007 for all apatites and amphiboles, <0.00010 for all phlogopites and whole rocks.
[b] The 2σ error is always <0.00003.

radiogenic Pb does not exceed 4% of the observed ratios (compare Kwon et al., 1989).

5. Discussion

5.1. The primary magmatic isotope signature

We obtained in most cases different oxygen isotope ratios for whole rock samples and carbonates separated from them. This was probably caused by different carbonate generations as revealed by CL microscopy. The almost identical isotope composition of all mineral separates from Tiksheozero in contrast to the scattering oxygen isotope values of corresponding whole rock samples can be explained by a preferred isotopic exchange in alteration zones, located mainly along grain boundaries, removed during the process of mineral separation, e.g., crushing, sieving and hand picking. The

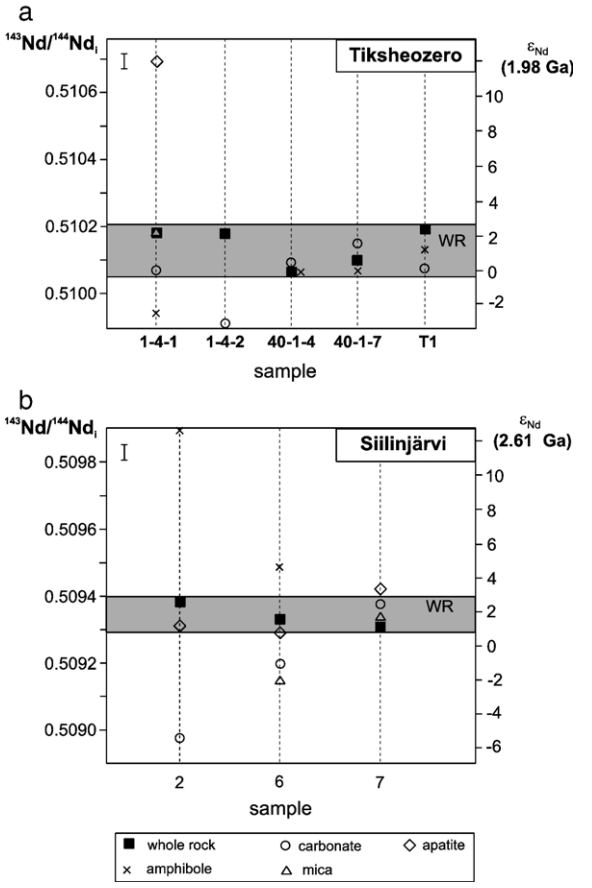

Fig. 6. Calculated initial Nd isotope ratios for whole rocks and separated minerals from Tiksheozero (a) and Siilinjärvi (b) carbonatite complexes. Error bar is given in the upper left corner. The grey field marks the variation determined for whole rock samples.

slightly higher oxygen isotope composition obtained from whole-rock samples by Tikhomirova et al. (1993; field T in Fig. 3a) can be explained by a mixture of different carbonate generations (e.g., cc-1 and cc-2).

Based on the uniform isotope composition and oxygen isotope temperatures we consider the carbon and oxygen isotope composition of carbonate separates with calcite reaction time as the primary magmatic signature for the Tiksheozero carbonatite. For the Siilinjärvi carbonatite, sample 5 best represents the primary igneous stable isotope composition of the early carbonatite melt judging from oxygen isotope temperatures and the almost unaltered idiomorphic to hypidiomorphic texture of the carbonatite matrix (Fig. 2e). Demeny et al. (2004) analysed other samples from Siilinjärvi, where the sample with the lowest oxygen isotope ratio yields almost the same $\delta^{18}O$ and $\delta^{13}C$ values (7.4‰ and −3.9‰, respectively). The calculated oxygen isotope temperature of the primary carbonate from Tiksheozero with amphibole and magnetite yields about 600 °C. Therefore, amphibole and magnetite in connection with primary calcite are best suited for the determination of the isotope temperature of carbonatite melts. Our results confirm those from Haynes et al. (2003) who found that calcite–magnetite oxygen isotope temperatures are generally the highest obtained in carbonatite complexes and represent crystallization temperatures of carbonatite magmas.

It is generally believed that the Sr and Nd isotope composition of carbonatites cannot be altered due to their high Sr and Nd concentrations. However, interaction with fluids at sub-solidus conditions have to be taken into consideration since these can carry high concentrations of Rb, Sr, and REE (e.g., Sindern and Kramm, 2000; Bühn et al., 2003; Marks et al., 2003). The initial $^{87}Sr/^{86}Sr$ isotope composition is best defined by pure mineral separates of calcite and apatite, and apatite seems to retain the initial Sr isotope ratio better (compare Section 5.2). Additional oxygen isotope

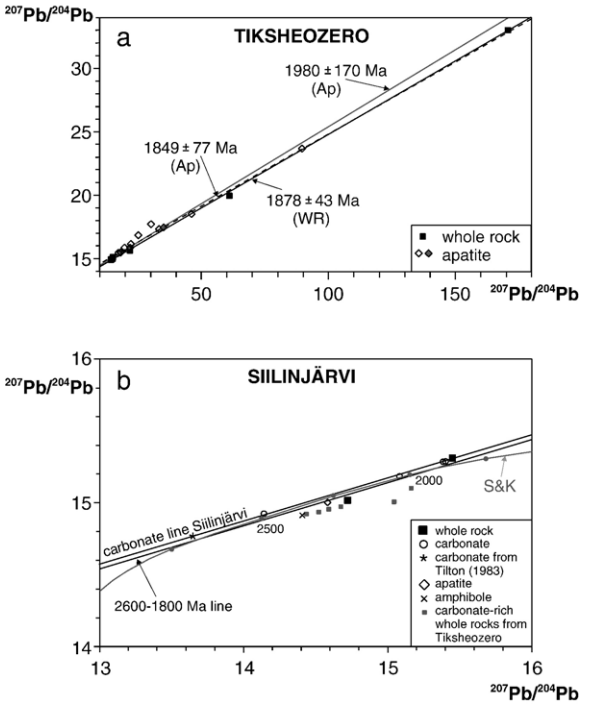

Fig. 7. (a) Lead isotope data for whole rocks and separated apatites from Tiksheozero carbonatite complex. For comparison published data from three apatites analysed by Shchiptsov et al. (1991) are shown as grey symbols and a grey isochron line. (b) Calculated initial (T=2.61 Ga) lead isotope data for whole rocks and mineral separates from the Siilinjärvi carbonatite complex, compared to data from Tilton (1983). In addition, the lowest uncorrected lead isotope data from Tiksheozero carbonate-rich whole rocks are given. S and K is the Stacey and Kramers (1975) evolution curve. See text for discussion.

analyses of these minerals are a good indicator for alteration processes. The variation of the initial Sr isotope composition of calcites and apatites from Tiksheozero carbonatites is similar to that reported by Zaitsev and Bell (1995) and Bizarro et al. (2003) within carbonatite samples interpreted by mantle heterogeneity. Mica seems to undergo the greatest disturbance in the Rb/Sr system during metamorphic overprint resulting in younger Rb/Sr isochron ages and too low calculated initial Sr isotope ratios. Nonetheless, the initial Sr isotope ratio of most whole rocks is preserved as indicated by values similar to those from apatites and calcites.

Distortion was also found in the Sm/Nd isotope system as indicated by younger mineral isochron ages compared to whole rock ages as well as scattered calculated ε_{Nd} values (compare Fig. 6). The lowest scatter in initial Nd isotope ratios was obtained from whole rocks and apatites which seem to be less affected of possible redistribution of rare earth elements during sub-solidus and/or metamorphic processes probably due to their high Nd concentrations.

In the U/Pb system, carbonates have the lowest U contents; therefore, their Pb/Pb ratios provide the best estimate for the primary Pb isotope composition of the investigated carbonatite complexes.

5.2. Late-stage sub-solidus processes

5.2.1. Effect of late-stage sub-solidus processes on the isotope composition

5.2.1.1. Carbonatites. Dolomites and many whole rocks from Tiksheozero and Siilinjärvi show elevated oxygen isotope composition (trend A in Fig. 3a and b) with almost identical $\delta^{13}C$ values. The identical C isotope ratios show, that the higher O isotope ratios are not the result of lower formation temperatures since this would increase both O and C isotope ratios (in isotopic equilibrium with carbonatite melt). Instead, this trend can be explained by interaction with a water-rich fluid. Keppler (2003) showed experimentally the very high water solubility of carbonatite melts. The decrease of water solubility in carbonatite melts at lower pressures (Keppler, 2003) explains why hydrothermal alteration (e.g., fenitization) is much stronger around shallow carbonatite intrusions and only weakly developed around deep intrusions. The two Karelian complexes present the deeper parts of carbonatite complexes, where fenitization produced only narrow zones around carbonatites. Nonetheless, even at these deeper parts of carbonatite complexes the oxygen isotope composition reports water release and fluid movement during ascent and emplacement.

Assuming an identical isotope composition for this water-rich fluid with that of the primary calcite (6.9‰), the mean $\delta^{18}O$ value for carbonate separates with dolomite reaction time (9.2‰) and for the carbonate separate with the highest $\delta^{18}O$ ratio (12‰) corresponds to isotope temperatures of about 500 °C and about 300 °C, respectively (O'Neil et al., 1969).

In the Sr isotope system, one carbonate separate of Tiksheozero carbonatites (red calcite of sample 169-79) shows a clear influence of sub-solidus processes proved by its elevated oxygen isotope composition (9.9‰). Its Sr concentration is distinctly lower than that of all other carbonates whereas its initial Sr ratio is clearly higher than that of the corresponding apatite (Fig. 5). Hence, in addition to mantle heterogeneity sub-solidus processes explain some of the observed scatter in the Sr isotope composition of the Tiksheozero carbonatites. The large scatter of initial Sr ratios of the Siilinjärvi carbonatites may at least partly be ascribed to late-stage interaction with water-rich fluids since there is a general tendency of decreasing Sr concentrations with increasing oxygen isotope composition (Fig. 8). These data indicate that calcite is more susceptible to alteration compared to apatite although most calcites have higher Sr concentrations (Fig. 5).

Our isotope data are not sufficient to judge if and how these sub-solidus processes can influence the Nd and Pb isotope composition of carbonatites.

5.2.1.2. Carbonatized silicic rocks. Carbonatized silicic rocks from Tiksheozero are different to carbonatites both in their O and C isotope composition indicating disequilibrium conditions. Deines (1989) proposed the Rayleigh fractionation model to cause the correlated increase of O and C isotope ratios observed in many carbonatite complexes especially for the formation of late-stage dolomitic and ankeritic carbonates corresponding to trend B in Fig. 3a. The oxygen isotope fractionation between silicate and oxide minerals (amphibole, magnetite) and calcite in carbonatized silicic rocks of Tiksheozero gives a rough temperature estimate for this process of about 400 °C (Tikhomirova et al., 1993).

Siilinjärvi glimmerites show lower carbon isotope ratios compared to the carbonatites (Fig. 3b). This behaviour (lower carbon isotope ratios for carbonatized silicic rocks) is rather unusual although Knudsen and Buchardt (1991) observed a similar tendency in late-stage sövite veins of the Qaqarssuk Carbonatite Complex, West Greenland. They explained the lower

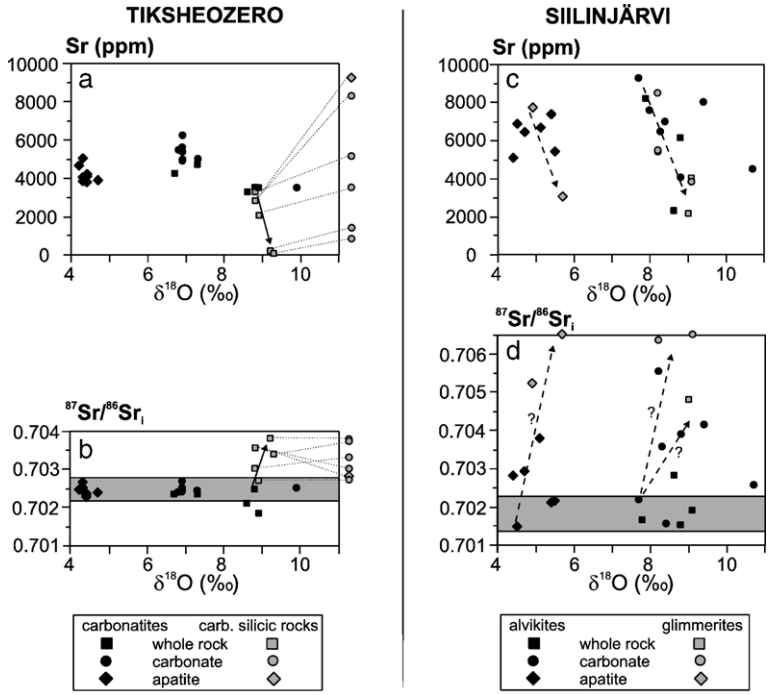

Fig. 8. Sr concentrations and Sr initial ratios versus oxygen isotope ratios for separated carbonates, apatites and whole rocks from Tiksheozero (a, b) and Siilinjärvi carbonatite (c, d) complexes. Sr data of samples from carbonatized silicic rocks of the Tiksheozero complex are shown as grey symbols. Symbols are shown at the right-hand side of the diagram if no oxygen isotope composition is available whereby tie lines join whole rocks and minerals from the same sample. Arrows indicate a tendency towards lower Sr concentrations and higher Sr isotope compositions for carbonatized silicic rocks from Tiksheozero. Corresponding carbonates also have mainly lower Sr concentrations and higher Sr isotope composition compared to those from carbonatites. Further possible trends are given for Siilinjärvi apatites and carbonates towards lower Sr concentrations and higher initial Sr isotope compositions with higher oxygen isotope ratios. Grey fields mark the primary magmatic Sr isotope composition determined by apatites and carbonates from borehole samples (b) and by the two samples with the lowest initial Sr isotope ratio for apatite and carbonate (d).

carbon isotope composition of these veins by the fractionation of heavy carbon into a gas phase. CO_2 degassing would lead to a combined decrease of carbon and oxygen isotope ratios since both ^{13}C and ^{18}O are enriched in the gas phase. The trend observed in our samples (Fig. 3b, trend B) can be explained by combination of CO_2 degassing (decreasing $\delta^{13}C$) and interaction with water-rich fluids (increasing $\delta^{18}O$).

Tiksheozero carbonatized silicic whole rocks and most of their calcites have lower Sr and higher Rb concentrations than carbonatite samples (Table 2b) but increased Sr isotope ratios (Fig. 8). We attribute this to interaction with a water-rich late-stage fluid (probably released during emplacement of the carbonatites) since there is a correlated increase of whole rock oxygen isotope ratios (Fig. 8).

Calcites and apatites from Siilinjärvi glimmerites have higher Sr initial ratios compared to those from alvikites. There seems to be a general trend of decreasing Sr concentrations with increasing $\delta^{18}O$ values for apatites, carbonates and whole rock samples (Fig. 8). For apatites (and probably also for carbonates) there is also a general trend towards higher $^{87}Sr/^{86}Sr$ with increasing $\delta^{18}O$ values (Fig. 8). Therefore, most of the primary igneous Sr isotope composition in Siilinjärvi apatites and carbonates seems to be lost during alteration processes.

5.2.2. Fluid-related element mobilization deduced from CL microscopy

The brighter and yellow CL colour of altered calcite (cc-2 in Tiksheozero and cc-3 of the cc-do-3 generation in Siilinjärvi) is probably related to lower Fe and/or higher REE and/or lower Mn concentrations (Machel, 2000; Habermann et al., 2000) redistributed during fluid transport. Simultaneously, the CL colour of apatite changes from violet in core regions to blue on their rims and fractures (Fig. 2d). Blue CL of apatite is related to Eu^{2+} whereas lilac-violet CL is caused by activation due to Ce^{3+} (e.g., Mitchell et al., 1997). Koberski and Keller (1995) have shown that decreasing REE contents in apatites resulted in a change of the CL colour of apatite from blue-violet to green. We attribute the bright yellow CL colour of cc-2 not to lower Mn or Fe contents, since this carbonate would liberate CO_2 during short reaction

time (calcite reaction time), but to an increase in their REE contents. This would also affect the Nd isotope system.

5.3. Changes related to the metamorphic overprint

Both Precambrian carbonatite complexes underwent a severe regional metamorphic overprint. The mineral and mica Rb/Sr isochron ages from Tiksheozero samples reflect resetting of mica due to activation of the Neoarchaean junction zone proceeding up to 1700 Ma. All Rb/Sr isochrons from Siilinjärvi samples yield ages that coincide with the formation of the Svecofennian Orogen. The Siilinjärvi mica isochron reports activity up to 1770 Ma. Some inheritance is indicated by older Rb/Sr ages, e.g., that of using large phlogopite phenocrysts from Tiksheozero sample 169-81 (1906 Ma, Fig. 4). Probably, the metamorphic overprint caused some scatter of the $\delta^{18}O$ values of mica whereas amphibole, magnetite and separated carbonates from borehole samples in large carbonatite bodies retain their primary oxygen values. It is not clear if the partial distortion of the Sm/Nd isotope system was caused by autometasomatic processes or due to the metamorphic overprint.

The secondary Pb/Pb isochrons from Tiksheozero and Siilinjärvi samples represent metamorphic ages. Probably, mobilization of uranium caused the high radiogenic Pb contents of the apatites and resulted in the reset of their U/Pb system. Decay-corrected initial Pb ratios of four carbonate mineral separates from Siilinjärvi define a line (Fig. 7b) together with one carbonate sample analysed by Tilton (1983). This carbonate line lies slightly above the growth curve of Stacey and Kramers (1975). When this line is moved towards lower $^{207}Pb/^{204}Pb$ ratios so that the lower intersect with the growth curve is at about 2600 Ma (the formation age), the upper intercept yields about 1800 Ma and may be related to the Svecofennian overprint (Fig. 7b). The carbonate sample with the lowest U content reported by Tilton (1983) has the least radiogenic Pb isotope ratio and was probably least affected by the metamorphic overprint.

5.4. Carbonatite mantle sources

5.4.1. Stable isotope composition (O, C)

Both carbonatite complexes show a remarkably uniform primary oxygen and carbon isotope composition (Tiksheozero: $\delta^{13}C=-5.0‰$, $\delta^{18}O=6.9‰$; Siilinjärvi: $\delta^{13}C=-3.7‰$, $\delta^{18}O=7.4‰$). This is different from many other carbonatite complexes where scattering O and C isotope values were obtained (e.g., Khibina complex: Zaitsev, 1996; Kovdor complex: Zaitsev and Bell, 1995; other complexes: Demeny et al., 2004). However, if different generations of carbonatites are compared in such complexes, early generations mostly define a very narrow field in their O and C isotope composition (e.g., Zaitsev, 1996; Demeny et al., 2004). Mainly the late carbonatite generations are influenced by Rayleigh fractionation processes resulting in increasing $\delta^{13}C$ and $\delta^{18}O$ values in vertical sections towards the surface as shown for Khibina carbonatites (Zaitsev, 1996). In addition, volcanic and sub-volcanic carbonatites are known to show a much larger scatter and more elevated oxygen isotope values in comparison to deep-seated carbonatite complexes (e.g., Deines and Gold, 1973; Samoilov and Plyusnin, 1982). Probably, this is mainly related to the larger role of fluid release from carbonatite melts at lower pressures. The homogeneous O and C isotope composition of Tiksheozero and Siilinjärvi carbonatites can be explained by discriminating the primary isotope composition from that related to sub-solidus exchange processes, and the absence of Rayleigh fractionation processes. Therefore, the first carbonate generation formed due to batch crystallization without significant isotope fractionation.

The oxygen isotope composition of mantle-derived rocks is determined by the oxygen isotope composition of their source and the temperature-dependent mineral–melt fractionation. Unaltered mantle rocks (e.g., MORB, OIB) are known to have very constant oxygen isotope compositions (e.g., Harmon and Hoefs, 1995). Fairly uniform O isotope compositions (about 7 to 7.5‰) for early generations of carbonatites were demonstrated by Demeny et al. (2004) for carbonatites from the KAP. Our calcite separates from Tiksheozero and the lowest O isotope composition from Siilinjärvi carbonatites are in the same range. Fresh, unaltered lavas from Oldoinyo Lengai show even a slightly lower oxygen isotope composition (Keller and Hoefs, 1995: from 5.8 to 6.7‰). This defines a “Lengai Box” for mantle carbonatites that is even more restricted than the “Taylor Box”. Deines (1989) estimated a fractionation of about 2‰ between the source (mantle peridotite) and the calcite at about 1000 °C. Therefore, the source oxygen isotope composition should lie in the range between 5 and 5.5‰, what is in good agreement with well established values from MORB and OIB (Harmon and Hoefs, 1995; 5.7‰ and 5.5‰, respectively).

The primary C isotope values of Siilinjärvi carbonatites are increased compared to the Taylor box (Fig. 3b). The comparison of mean $\delta^{13}C$ values of various carbonatite complexes using only carbonates with

$\delta^{18}O$ values between 5.5 and 8.5‰ shows, that many carbonatite complexes show higher than mantle $\delta^{13}C$ values (i.e. higher than −4‰ according to Taylor et al., 1967), although the mean carbon isotope composition of all carbonatites is in the range of mantle material (Deines, 1989: −5.5‰). Ray et al. (1999) argued, that these higher $\delta^{13}C$ values are an indication for recycled crustal inorganic carbon (average $\delta^{13}C = 0$‰) into the mantle source region. This explanation would require substantial recycling of crustal carbonates for the Archaean Siilinjärvi complex. However, recycling of crustal carbonates into the mantle would cause simultaneous enrichment of ^{18}O and shifts in other isotope systems (Sr, Nd, Pb) in the source, which is not observed. There is also no tendency of increased $\delta^{13}C$ values for younger carbonatite complexes worldwide which would be expected from repeated recycling of crustal carbon since the Archaean. Therefore, we do not believe that crustal recycling is responsible for the elevated $\delta^{13}C$ values of the Siilinjärvi complex.

Whatever source(s) are proposed, the uniform $\delta^{13}C$ values of Tiksheozero and Siilinjärvi carbonatites as well as those analysed by Ray et al. (1999) require homogenization in the carbonatite melt probably occurring in the magma chamber, where the final carbon isotope compositions of carbonatite melt should be achieved. Then, isotope fractionation caused by disproportion of carbon into different phases in the magma chamber dependent on its local conditions (e.g., depth, pressure, redox conditions, storing time) probably better explains the differences in $\delta^{13}C$ values between different carbonatite complexes and carbonate generations of the same complex. This interpretation agrees with the carbon isotope geochemistry of mantle xenoliths, whose $\delta^{13}C$ variations are shown not to be caused by subduction of crustal carbon (Deines, 2002). Instead, the presence of two mantle components with different carbon isotope compositions (−5‰ and −25‰) and fractionation processes between different carbon phases (e.g., CH_4, C, CO, CO_2, carbon dissolved in silicate phases, SiC) are responsible for the observed mantle carbon isotope distribution (Deines, 2002). Such disproportion processes in the magma chamber can explain the different $\delta^{13}C$ composition of young oceanic carbonatites (Hoernle et al., 2002). The uniform $\delta^{18}O$ composition of unaltered carbonatites worldwide indicates an insignificant role of oxygen-bearing carbon phases during fractionation processes in the magma chamber.

5.4.2. Sr, Nd, and Pb isotope composition

Carbonatites usually define a linear array in a Sr–Nd isotope diagram interpreted to represent a mixing line between two endmembers: one depleted and one enriched (e.g., Bell and Blenkinsop, 1989). A compilation of all carbonatite data from KAP indicates at least three distinct endmembers in the Nd–Sr space: one depleted and two enriched ones (Bell and Rukhlov, 2004). Canadian carbonatites were first used to show that the depleted mantle source is long-lived and was formed about 3 Ga ago, and that Sr and Nd isotopes (Bell and Blenkinsop, 1989) as well as Pb isotopes (Kwon et al., 1989) are correlated. Isotope data from old carbonatites from other continents are still sparse. Nonetheless, Rukhlov et al. (2001) and Bell and Rukhlov (2004) compared Sr and Nd data from Canada, Fennoscandia and Greenland and they concluded that all data show the same features: depletion of Rb/Sr to 0.02 at about 3 Ga, and enrichment of Sm/Nd in this source well before 3 Ga (compare Fig. 9a, b). In this compilation only the lowest initial $^{87}Sr/^{86}Sr$, and the highest $\varepsilon_{Nd}(T)$ values are indicative of the depleted source since most alteration processes (especially interaction with crustally derived components) cause an increase of the $^{87}Sr/^{86}Sr_i$ and a decrease of ε_{Nd}.

Although many of our isotope data are disturbed due to autometasomatic sub-solidus exchange and/or metamorphic processes we can use the least disturbed phases and samples (compare Section 5.1) with lowest values for Sr and Pb isotopes and highest values for Nd isotopes for comparison with the evolution lines for the depleted mantle source (Fig. 9).

The lowest Sr isotope ratios of our carbonates and apatites from the Archaean Siilinjärvi and the Palaeoproterozoic Tiksheozero complexes are in the range of bulk silicate Earth (BSE) with a Rb/Sr ratio of 0.03 and higher than Canadian carbonatites of similar ages (Fig. 9a). One sample from the 1.9 Ga alkaline complex Gremyakha–Vyrmes has a slightly lower initial Sr isotope ratio than BSE (Fig. 9a, data from Savatenkov et al., 1999). Although the model of Bell and Rukhlov (2004) may be also valid for Fennoscandia, we propose a slightly different model with a continuous decrease in Rb/Sr ratio (compare Fig. 9a) which better explains the slightly higher values for Precambrian Fennoscandian carbonatites compared to those of Canada. The decrease in the Rb/Sr ratio was probably only weak during the first crust-forming event at 3.2–3.0 Ga in the Karelian Craton (Hölttä et al., 2000), but should be essential during the extensive crust-forming event at 2.87–2.65 Ga (Bibikova et al., 2001) leading to a difference in the Fennoscandian mantle isotope evolution line (black broken line in Fig. 9a) compared to that for the bulk Earth.

Our Nd data from Siilinjärvi and Tiksheozero are in agreement with the conclusion of Bell and Rukhlov (2004) that the Nd isotope composition of early Precambrian carbonatites from Fennoscandia is higher than CHUR (chondritic uniform reservoir). The carbonatite veins of the Gremyakha–Vyrmes complex also show positive ε_{Nd} values up to +2.2 (Savatenkov et al., 1999). This observation coincides with results of Vrevsky et al. (2003) on Archaean komatiites from the Baltic shield. Most komatiites yield positive ε_{Nd} values which differed in time and space during the Archaean together with their REE pattern. Therefore, the asthenospheric mantle was even during Archaean times both laterally and vertically heterogeneous in its Nd isotope composition and REE pattern. Vrevsky et al. (2003) explained this with garnet fractionation in the mantle due to early Archaean oceanic crust forming events in connection with plume evolution.

Pb isotope data are essential in recognizing early mantle depletion of uranium because the short half-life of ^{235}U makes the $^{207}Pb/^{204}Pb$ ratio sensitive to Archaean U/Pb differentiation. Kwon et al. (1989) found that almost all carbonatites from Canada plot in a $^{206}Pb/^{204}Pb$–$^{207}Pb/^{204}Pb$ diagram below the isotope evolution curve of Stacey and Kramers (1975) due to early U depletion in the mantle source. In contrast, young carbonatites often show similarities to HIMU–OIB caused by U enrichment (or Pb depletion) in the source region. There is no indication for a HIMU component in both investigated Fennoscandian carbonatite complexes which would cause higher $^{206}Pb/^{204}Pb$ ratios compared to single-stage Pb isochrons. The Pb isotope composition of the Siilinjärvi carbonatite (Fig. 7B) does not indicate early Archaean U depletion in the source region to produce lower $^{207}Pb/^{204}Pb$ ratios. The position of the Siilinjärvi carbonate line slightly above the Stacey and Kramers (1975) curve can be explained by a higher μ ($^{238}U/^{204}Pb$) typical for Finnish compared to Canadian Archaean rocks (Tilton, 1983). In contrast, the lowest $^{206}Pb/^{204}Pb$ ratios of Tiksheozero carbonatites are lower than the crust evolution line (Fig. 9c,

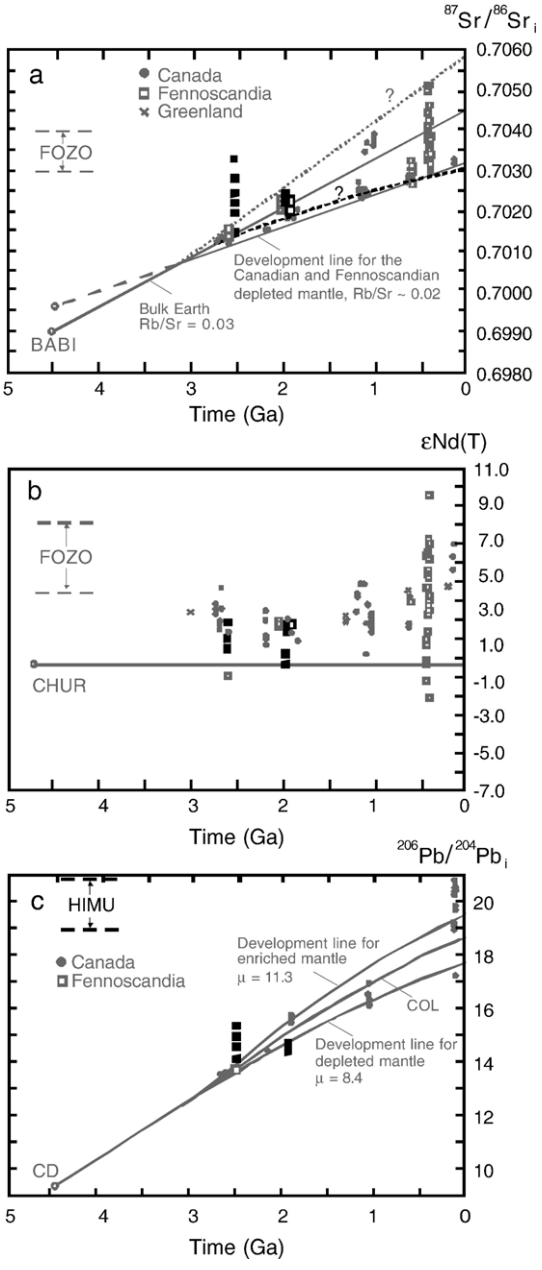

Fig. 9. Isotope development diagrams for carbonatites. (a) $^{87}Sr/^{86}Sr_i$ vs. time. Grey lines and data are from Bell and Rukhlov (2004) with BABI (basaltic achondritic best initial) as the initial isotopic composition of the primitive silicate Earth. FOZO (focus zone) represents the depleted mantle endmember. Black filled symbols present data from Siilinjärvi and Tiksheozero Complexes (this work). Black open symbols present data from Gremyakha–Vyrmes Complex (Savatenkov et al., 1999). Black broken line is the proposed development line for the Fennoscandian mantle – see text for discussion. (b) ε_{Nd} (T) vs. time. Grey lines and data are from Bell and Rukhlov (2004) with CHUR (chondritic uniform reservoir). FOZO (focus zone) represents the depleted mantle endmember. Black filled symbols present data from Siilinjärvi and Tiksheozero complexes (this work). Black open symbols present data from Gremyakha–Vyrmes Complex (Savatenkov et al., 1999). (c) $^{206}Pb/^{204}Pb_i$ vs. time. Grey lines and data are from Kwon et al. (1989) with CD (Canyon Diablo troilite), one evolution line for COL (conformable ore lead) similar to the Stacey and Kramers crustal growth curve, a second evolution line for an enriched mantle endmember leading to the HIMU isotope characteristics and a third evolution line for the depleted mantle endmember. Black filled symbols present data from Siilinjärvi and Tiksheozero complexes (this work).

COL) indicative of an already depleted (lower μ) mantle below Fennoscandia at about 2 Ga.

In conclusion, it seems possible that depletion of the mantle source regions occurred not simultaneously for the Rb/Sr, Sm/Nd and U/Pb system. In the Fennoscandian asthenospheric mantle the increase of the Sm/Nd ratio started in Archaean time (>3.1 Ga) probably due to formation of oceanic crust accompanied by mineral fractionation processes (e.g., garnet fractionation; Vrevsky et al., 2003), whereas the depletion of the Rb/Sr ratio probably was mainly initiated at about 2.9–2.6 Ga due to extensive continental crust formation. No indication for a Precambrian HIMU component was found in the two investigated complexes, but Tiksheozero carbonatites indicate the existence of a depleted mantle (lower μ) below Fennoscandia at about 2 Ga.

6. Conclusions

Large variations in the O, C, Sr, Nd and Pb isotope composition were found in the Precambrian Tiksheozero and Siilinjärvi carbonatite complexes from KAP. The combined approach of microscopic investigations using CL as well as stable and radiogenic isotopes on the same samples and mineral separates enabled us to identify the primary isotope composition as well as various processes that caused shifts in isotope systems. Primary isotope signatures are preserved in most calcites (O, C, Sr, Pb), apatites (O, Sr, Nd), amphibole (O), magnetite (O), and whole rocks (Sr, Nd).

The primary igneous C and O isotope composition is different for both complexes (Tiksheozero: $\delta^{13}C = -5.0‰$, $\delta^{18}O = 6.9‰$; Siilinjärvi: $\delta^{13}C = -3.7‰$, $\delta^{18}O = 7.4‰$) but very uniform. The lowest Sr isotope ratios of carbonates and apatites from the Archaean Siilinjärvi (0.70137) and the Palaeoproterozoic Tiksheozero (0.70228) complexes are in the range of bulk silicate Earth (BSE) and higher than those from Canadian carbonatites of similar ages. Therefore, the depletion of the Rb/Sr ratio of the Fennoscandian mantle probably occurred slightly later compared to that of the Canadian mantle, whereas the Nd isotope composition points to very early Archaean enrichment of Sm/Nd in both continents causing positive ε_{Nd} values. No HIMU components could be detected in the two complexes, whereas Tiksheozero carbonatites give the first indication of Palaeoproterozoic U depletion for Fennoscandia.

Acknowledgements

H. Vartianen is thanked for guidance in the Siilinjärvi open pit. V.V. Shchiptsov is thanked for providing borehole samples from the Tiksheozero complex. This study was funded by Deutsche Forschungsgemeinschaft (DFG) grant Ti 211/9. We are indebted to all co-workers from the Isotope Laboratory Freiberg for assistance with isotope work. Thorough reviews by R. Halama and K. Bell and constructive comments by G. Markl improved the quality of the paper substantially.

Appendix A. Supplementary data

Supplementary data associated with this article can be found, in the online version, at doi:10.1016/j.lithos.2006.03.019.

References

Bell, K., 1998. Radiogenic isotope constraints on relationships between carbonatites and associated silicate rocks – a brief review. J. Petrol. 39, 1987–1996.

Bell, K., Blenkinsop, J., 1989. Neodymium and strontium isotope geochemistry of carbonatites. In: Bell, K. (Ed.), Carbonatites – Genesis and Evolution. Unwin Hyman, London, pp. 278–300.

Bell, K., Rukhlov, A.S., 2004. Carbonatites from the Kola Alkaline Province: origin, evolution and source characteristics. In: Wall, F., Zaitsev, A.N. (Eds.), Phoscorites and Carbonatites from Mantle to Mine: The Key Example of the Kola Alkaline Province. Mineralogical Society Series, vol. 10. Mineralogical Society of Great Britain & Ireland, London, pp. 433–468 (Printed and bound by Black Bear Press, Cambridge).

Bell, K., Tilton, G.R., 2001. Nd, Pb and Sr isotopic compositions of East African carbonatites: evidence for mantle mixing and plume inhomogeneity. J. Petrol. 42, 1927–1945.

Bibikova, E.V., Slabunov, A.I., Kirnozova, T.I., Makarov, V.A., 1997. U–Pb geochronology and major-element chemistry of a diorite–plagiogranite batholith in Northern Karelia. Geochem. Int. 11, 1154–1160.

Bibikova, E., Skiöld, T., Bogdanova, S., Gorbatschev, R., Slabunov, A., 2001. Titanite–rutile thermochronometry across the boundary between the Archaean Craton in Karelia and the Belomorian Mobile Belt, eastern Baltic Shield. Precambrian Res. 105, 315–330.

Bizarro, M., Simonetti, A., Stevenson, R.K., Kurszlaukis, S., 2003. In situ $^{87}Sr/^{86}Sr$ investigation of igneous apatites and carbonates using laser-ablation MC–ICP–MS. Geochim. Cosmochim. Acta 67, 289–302.

Borthwick, J., Harmon, R.S., 1982. A note regarding ClF_3 as an alternative to BrF_5 for oxygen isotope analysis. Geochim. Cosmochim. Acta 46, 1665–1668.

Bottinga, Y., Javoy, M., 1975. Oxygen isotope partitioning among the minerals in igneous and metamorphic rocks. Rev. Geophys. Space Phys. 13, 401–418.

Bühn, B., Schneider, J., Dulski, P., Rankin, A.H., 2003. Fluid–rock interaction during progressive migration of carbonatitic fluids, derived from small-scale trace element and Sr, Pb isotope distribution in hydrothermal fluorite. Geochim. Cosmochim. Acta 67, 4577–4595.

Chiba, H., Chacko, T., Clayton, R.N., Goldsmith, J.R., 1989. Oxygen isotope fractionations involving diopside, forsterite, magnetite, and calcite: application to geothermometry. Geochim. Cosmochim. Acta 53, 2985–2995.

Cole, D.R., Horita, J., Polyakov, V.B., Valley, J.W., Spicuzza, M.J., Coffey, D.W., 2004. An experimental and theoretical determination of oxygen fractionation in the system magnetite–H_2O from 300 to 800 °C. Geochim. Cosmochim. Acta 68, 3569–3585.

Deines, P., 1989. Stable isotope variations in carbonatites. In: Bell, K. (Ed.), Carbonatites – Genesis and Evolution. Unwin Hyman, London, pp. 301–359.

Deines, P., 2002. The carbon isotope geochemistry of mantle xenoliths. Earth-Sci. Rev. 58, 247–278.

Deines, P., Gold, D.P., 1973. The isotope composition of carbonatite and kimberlite carbonates and their bearing on the isotopic composition of deep-seated carbon. Geochim. Cosmochim. Acta 37, 1709–1733.

Demeny, A., Sitnikova, M.A., Karchevsky, P.I., 2004. Stable C and O isotope compositions of carbonatite complexes of the Kola Alkaline Province: phoscorite–carbonatite relationships and source compositions. In: Wall, F., Zaitsev, A.N. (Eds.), Phoscorites and Carbonatites from Mantle to Mine: The Key Example of the Kola Alkaline Province. Mineralogical Society Series, vol. 10. Mineralogical Society of Great Britain & Ireland, London, pp. 407–431 (Printed and bound by Black Bear Press, Cambridge).

Fortier, S.M., Lüttge, A., 1995. An experimental calibration of the temperature dependence of oxygen isotope fractionation between apatite and calcite at high temperatures (350–800 °C). Chem. Geol. 125, 281–290.

Fortier, S.M., Lüttge, A., Satir, M., Metz, P., 1994. Oxygen isotope fractionation between fluorphlogopite and calcite: an experimental investigation of temperature dependence and F^-/OH^- effects. Eur. J. Mineral. 6, 53–65.

Habermann, D., Neuser, R.D., Richter, D.K., 2000. Quantitative high resolution spectral analysis of Mn^{2+} in sedimentary calcite. In: Pagel, M., Barbin, V., Blanc, P., Ohnenstetter, D. (Eds.), Cathodoluminescence in Geosciences. Springer Verlag, Berlin, pp. 331–358.

Halama, R., Vennemann, T., Siebel, W., Markl, G., 2005. The Gronnedal–Ika carbonatite–syenite complex, South Greenland: carbonatite formation by liquid immiscibility. J. Petrol. 46, 191–217.

Harmon, R.S., Hoefs, J., 1995. Oxygen isotope heterogeneity of the mantle deduced from global ^{18}O systematics of basalts from different geotectonic settings. Contrib. Mineral. Petrol. 120, 95–114.

Haynes, E.A., Moecher, D.P., Spicuzza, M.J., 2003. Oxygen isotope composition of carbonates, silicates, and oxides in selected carbonatites: constraints on crystallization temperatures of carbonatite magmas. Chem. Geol. 193, 43–57.

Herms, P., 1986. Petrologische und geochemische Untersuchung des Karbonatit–Glimmerit–Komplexes von Siilinjärvi, Finnland, und seines fenitisierten Rahmens. Dr. thesis, University of Kiel, unpublished.

Hölttä, P., Huhma, H., Mänttäri, I., Paavola, J., 2000. *P–T–t* development of Archaean granulites in Varpaisjärvi, Central Finland: II. Dating of high-grade metamorphism with the U–Pb and Sm–Nd methods. Lithos 50, 121–136.

Hoernle, K., Tilton, G., LeBas, M.J., Duggen, S., Garbe-Schönberg, D., 2002. Geochemistry of oceanic carbonatites compared with continental carbonatites: mantle recycling of oceanic crustal carbonate. Contrib. Mineral. Petrol. 142, 520–542.

Keller, J., Hoefs, J., 1995. Stable isotope characteristics of recent natrocarbonatites from Oldoinyo Lengai. In: Bell, K., Keller, J. (Eds.), Carbonatite Volcanism: Oldoinyo Lengai and the Petrogenesis of Natrocarbonatites. Springer Verlag, Berlin, pp. 113–123.

Keppler, H., 2003. Water solubility in carbonatite melts. Am. Mineral. 88, 1822–1824.

Klyunin, S.F., Panichev, V.V., 1987. Geological building and mineral resources from the Panaryarvin zone and its framework. North-West Geological Survey. Reprint, Monchegorsk (in Russian).

Knudsen, C., Buchardt, B., 1991. Carbon and oxygen isotope composition of carbonates from the Qaqarssuk Carbonatite Complex, southern West Greenland. Chem. Geol. 86, 263–274.

Koberski, U., Keller, J., 1995. Cathodoluminescence observations of natrocarbonatites and related peralkaline nephelinites at Oldoinyo Lengai. In: Bell, K., Keller, J. (Eds.), Carbonatite Volcanism: Oldoinyo Lengai and the Petrogenesis of Natrocarbonatites. Springer Verlag, Berlin, pp. 87–99.

Kontinen, A., Paavola, J., Lukkarinen, H., 1992. K–Ar ages of hornblende and biotite from Late Archaean rocks of eastern Finland – interpretation and discussion of tectonic implications. Geol. Surv. Finl., Bull. 365.

Kramm, U., 1993. Mantle components of carbonatites from the Kola Alkaline Province, Russia and Finland: a Nd–Sr study. Eur. J. Mineral. 5, 985–989.

Kwon, S.-T., Tilton, G.R., Grünenfelder, M.H., 1989. Lead isotope relationships in carbonatites and alkalic complexes: an overview. In: Bell, K. (Ed.), Carbonatites – Genesis and Evolution. Unwin Hyman, London, pp. 360–387.

Machel, H.G., 2000. Application of cathodoluminescence to carbonate diagenesis. In: Pagel, M., Barbin, V., Blanc, P., Ohnenstetter, D. (Eds.), Cathodoluminescence in Geosciences. Springer Verlag, Berlin, pp. 271–301.

Manhes, G., Minster, J.F., Allegre, C.J., 1978. Comparative uranium–thorium–lead and rubidium–strontium study of the Saint Severin amphoterite; consequences for early solar system chronology. Earth Planet. Sci. Lett. 39, 14–24.

Marks, M., Vennemann, T., Siebel, W., Markl, G., 2003. Quantification of magmatic and hydrothermal processes in a peralkaline syenite – alkali granite complex based on textures, phase equilibria, and stable and radiogenic isotopes. J. Petrol. 44, 1247–1280.

McCrea, J.M., 1950. On the isotopic chemistry of carbonates and a paleotemperature scale. J. Chem. Phys. 18, 849–857.

Mitchell, R.H., Xiong, J., Mariano, A.N., Fleet, M.E., 1997. Rare-earth-element-activated cathodoluminescence in apatite. Can. Mineral. 35, 979–998.

Nelson, D.R., Chivas, A.R., Chappell, B.W., McCulloch, M.T., 1988. Geochemical and isotopic systematics in carbonatites and implications for the evolution of ocean–island sources. Geochim. Cosmochim. Acta 52, 1–17.

Neuser, R.D., Bruhn, F., Götze, J., Habermann, D., Richter, D.K., 1995. Cathodoluminescence: method and application. Zentralbl. Geol. Paläontol., Teil I H ½, 287–306.

Nironen, M., 1997. The Svecofennian Orogen: a tectonic model. Precambrian Res. 86, 21–44.

O'Neil, J.R., Clayton, R.N., Mayeda, T.K., 1969. Oxygen isotope fractionation in divalent metal carbonates. J. Chem. Phys. 51, 5547–5558.

Patchett, P.J., Kuovo, O., Hedge, C.E., Tatsumoto, M., 1981. Evolution of continental crust and mantle heterogeneity: evidence from Hf isotopes. Contrib. Mineral. Petrol. 78, 279–297.

Puustinen, K., 1971. Geology of the Siilinjärvi carbonatite complex, Eastern Finland. Bull. Comm. Geol. Finl. 249, 1–43.

Puustinen, K., 1972. Richterite and actinolite from the Siilinjärvi carbonatite complex, Finland. Bull. Geol. Soc. Finl. 44, 83–86.

Ray, J.S., Ramesh, R., 1998. Stable carbon and oxygen isotope analysis of natural calcite and dolomite mixtures using selective acid extraction. J. Geol. Soc. India 52, 323–332.

Ray, J.S., Ramesh, R., Pande, K., 1999. Carbon isotopes in Kergulen plume-derived carbonatites: evidence for recycled inorganic carbon. Earth Planet. Sci. Lett. 170, 205–214.

Rukhlov, A., Bell, K., Ivanikov, V., 2001. Archean mantle below the Baltic Shield: isotopic evidence from intrusive carbonatites. J. Afr. Earth Sci. 32, A30–A31.

Samoilov, V.S., Plyusnin, G.S., 1982. The source of material for rare-earth carbonatites. Geochem. Int. 19 (5), 13–25.

Savatenkov, V.M., Pushkarev, Yu.D., Sergeyev, A.V., Sulimov, R.B., 1999. Carbonatites as an indicator of new ore types in the Gremyakha–Vyrmes Massif, Russia. Geol. Rudn. Mestorozhd. 41, 449–454 (in Russian).

Shchiptsov, V.V., Tson, O.V., Zheldakov, Yu.A., 1991. The distribution of U–Th–Pb and rare earth elements in apatites of Karelia. Mineral. Zh. 13 (4), 92–98 (in Russian).

Sindern, S., Kramm, U., 2000. Volume characteristics and element transfer of fenite aureoles: a case study from the Iivaara alkaline complex, Finland. Lithos 51, 75–93.

Stacey, J.S., Kramers, J.D., 1975. Approximation of terrestrial lead isotopic evolution by a two-stage model. Earth Planet. Sci. Lett. 26, 207–221.

Taylor, H.P., Frechen, J., Degens, E.T., 1967. Oxygen and carbon isotope studies of carbonatites from the Laacher See district, West Germany and the Alnö district, Sweden. Geochim. Cosmochim. Acta 31, 407–430.

Tikhomirova, M., Sallier, M.E., Safronova, G.P., 1993. Oxygen and carbon isotope variations of carbonates and silicates from the carbonatite massif Tiksheozero (Northern Karelia). Isotopenpraxis 28, 237–250.

Tichomirowa et al., in preparation. Zircon ages and geochemistry of carbonatites from Tiksheozero and Siilinjärvi, Kola Alkaline Province.

Tilton, G.R., 1983. Evolution of depleted mantle: the lead perspective. Geochim. Cosmochim. Acta 47, 1191–1197.

Tilton, G.R., Bell, K., 1994. Sr–Nd–Pb isotope relationships in Late Archean carbonatites and alkaline complexes: applications to the geochemical evolution of Archean mantle. Geochim. Cosmochim. Acta 58, 3145–3154.

Vrevsky, A.B., Matrenichev, V.A., Ruzheva, M.S., 2003. Petrology of komatiites from the Baltic Shield and isotope geochemical evolution of their mantle sources. Petrology 11, 532–561 (translated from Petrologiya).

Walters, L.J., Claypool, G.E., Choquette, P., 1972. Reaction rates and $\delta^{18}O$ variation for the carbonate–phosphoric acid preparation method. Geochim. Cosmochim. Acta 36, 129–140.

Zaitsev, A.N., 1996. Rhombohedral carbonates from carbonatites of the Khibina Massif, Kola peninsula, Russia. Can. Mineral. 34, 453–468.

Zaitsev, A.N., Bell, K., 1995. Sr and Nd isotope data of apatite, calcite and dolomite as indicators of source, and the relationships of phoscorites and carbonatites from the Kovdor Massif, Kola Peninsula, Russia. Contrib. Mineral. Petrol. 121, 324–335.

Zhao, G., Cawood, P.A., Wilde, S.A., Sun, M., 2002. Review of global 2.1–1.8 Ga orogens: implications for a pre-Rodinia supercontinent. Earth-Sci. Rev. 59, 125–162.